Electronic Supplementary Material (ESI) for RSC Advances.

Electronic Supplementary Information

A cationic water-soluble pillar[5]arene: synthesis and host-guest complexation with long linear acids

Gui-yuan Wu, Bing-bing Shi, Qi Lin, Hui Li, You-ming Zhang, Hong Yao, Tai-bao Wei*

Key Laboratory of Eco-Environment-Related Polymer Materials, Ministry of Education of China, Key Laboratory of Polymer Materials of Gansu Province, College of Chemistry and Chemical Engineering, Northwest Normal University, Lanzhou, Gansu, 730070, P. R. China.

Table of Contents

1 Materials and methods

1.1 Materials

Hydroquinone, boron trifluoride ethyl ether complex, 1,4-Dibromobutane, oxalic acid, butanedioic acid, adipic acid, and trimethylamine were reagent grade and used as received. Solvents were either employed as purchased or dried by $CaCl_2$. ^1H NMR spectra were recorded on a Mercury-400BB spectrometer at 400 MHz and ^{13}C NMR spectra were recorded on a Mercury-400BB spectrometer at 400 MHz. Chemical shifts are reported in ppm downfield from tetramethylsilane (TMS, δ scale with solvent resonances as internal standards). 2D ^1H-^1H NOESY spectrum was collected recorded on a Mercury-600BB spectrometer at 600 MHz. Melting points were measured on an X-4 digital melting-point apparatus (uncorrected). UV–vis spectra were recorded on a Shimadzu UV-2550 spectrometer. Fluorescence spectra were recorded on a Shimadzu RF-5310 spectrometer. Cyclic voltammetry (CV) was carried out using CHI660B (Shanghai Chen hua) potentiostat with a conventional three-electrode cell. Mass spectra were performed on a Bruker Esquire 3000 plus mass spectrometer (Bruker-Franzen Analytik GmbH Bremen, Germany) equipped with ESI interface and ion trap analyzer.

1.2 Determination of association constant

The association constants (Ka) of **P** and Guests were determined based on the absorbance titration curve using the equation as follows: where A_1 and A_0 represent the absorbance of host in the presence and absence of guests, respectively. A_{max} is the saturated absorbance of host in the presence of excess amount of guests; [G] is the concentration of [Guests] added.

$$\frac{1}{A_1-A_0} = \frac{1}{A_{max}-A_0}\left[\frac{1}{K_a[G]} + 1\right]$$

Synthesis of P

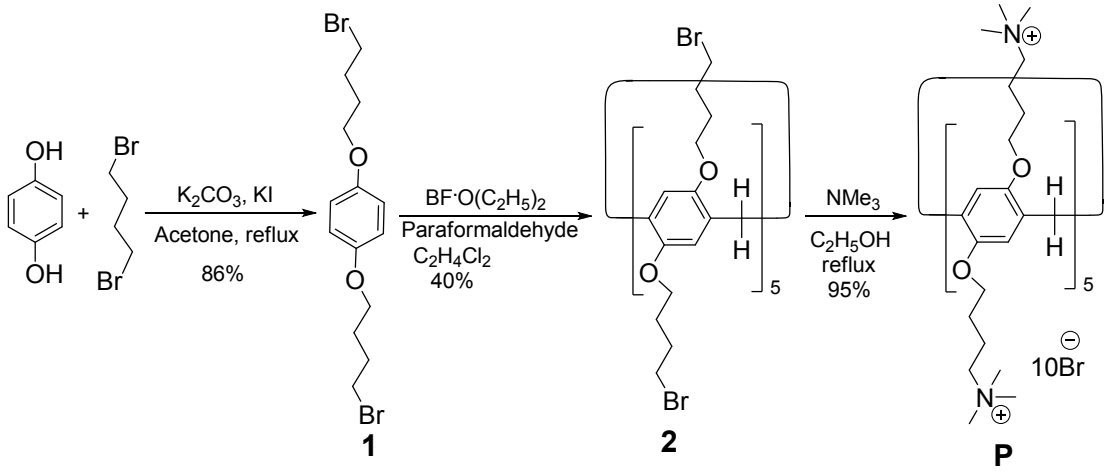

2.1 Synthesis of 1

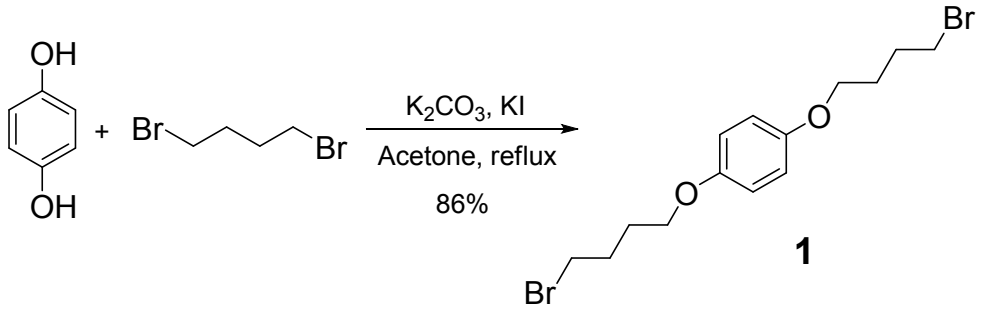

Hydroquinone (2.2 g, 20.0 mmol), K_2CO_3 (13.8 g, 100 mmol), KI (0.83 g, 5mmol), 1,4-Dibromobutane (17.28 g, 80.0 mmol) and acetone (200.0 mL) were added in a 250 mL round–bottom flask. The reaction mixture was stirred at reflux for 5 days. Then 200 mL of cold water was added to the reaction mixture, where product 1 precipitated as a white solid. The product was collected by vacuum filtration, thoroughly washed with water, and then naturaly air. The obtained solid was purified by column chromatography on silica gel with petroleum ether/ethyl acetate (5:1 *v*/*v*) as the eluent to get a white powder (6.5 g, 86 %). m.p. 86 °C. ^{1}H NMR (400MHz, $CDCl_3$) δ (ppm): δ 6.81 (s, 4H), 3.94 (dd, J = 10.0, 5.8 Hz, 4H), 3.48 (t, J = 6.6 Hz, 2H), 3.26 (t, J = 6.8 Hz, 2H), 2.09-1.85 (m, 8H). ^{13}C NMR (100 MHz, $CDCl_3$) δ: 153.08, 115.42, 67.37, 33.45, 30.22 , 29.49, 27.99. HRESIMS is shown in Fig S3: *m*/*z* calcd for $[M+H]^+$ $C_{14}H_{20}Br_2O_2$, 381.12; found 380.988.

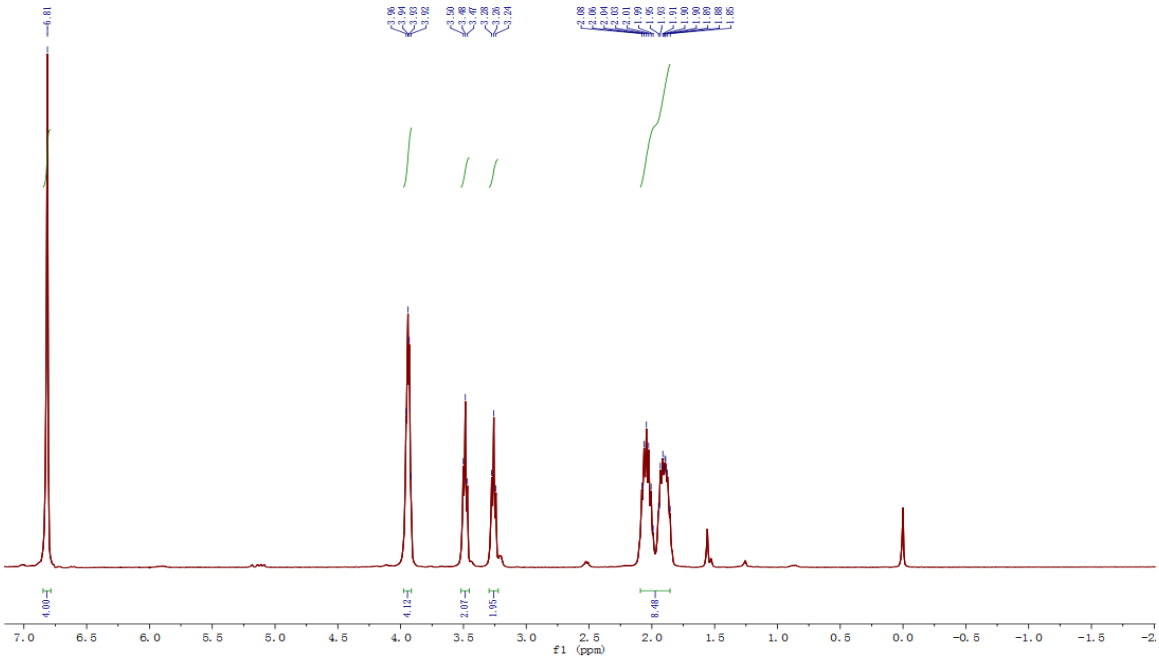

Fig. S1. ^{1}H NMR (400MHz, 298K) spectra of product 1 in $CDCl_3$.

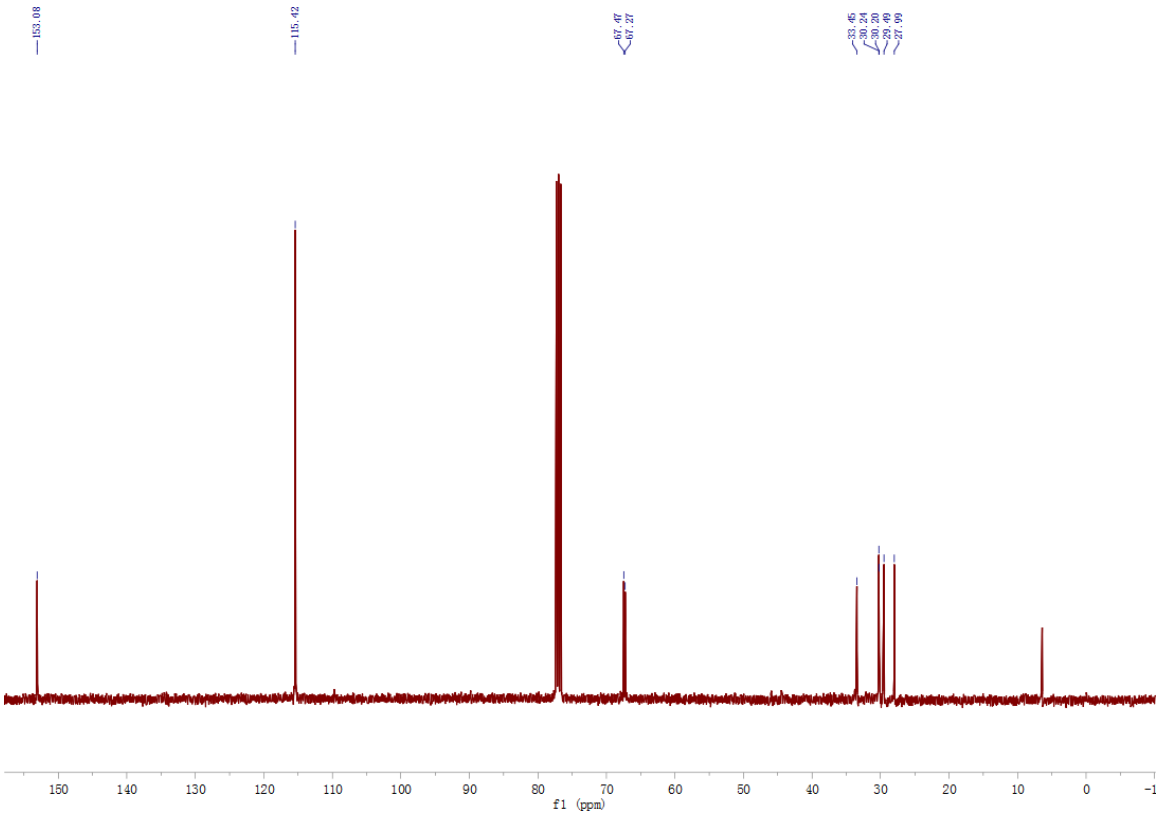

Fig. S2. ^{13}C NMR (400MHz, 298K) spectra of product 1 in $CDCl_3$.

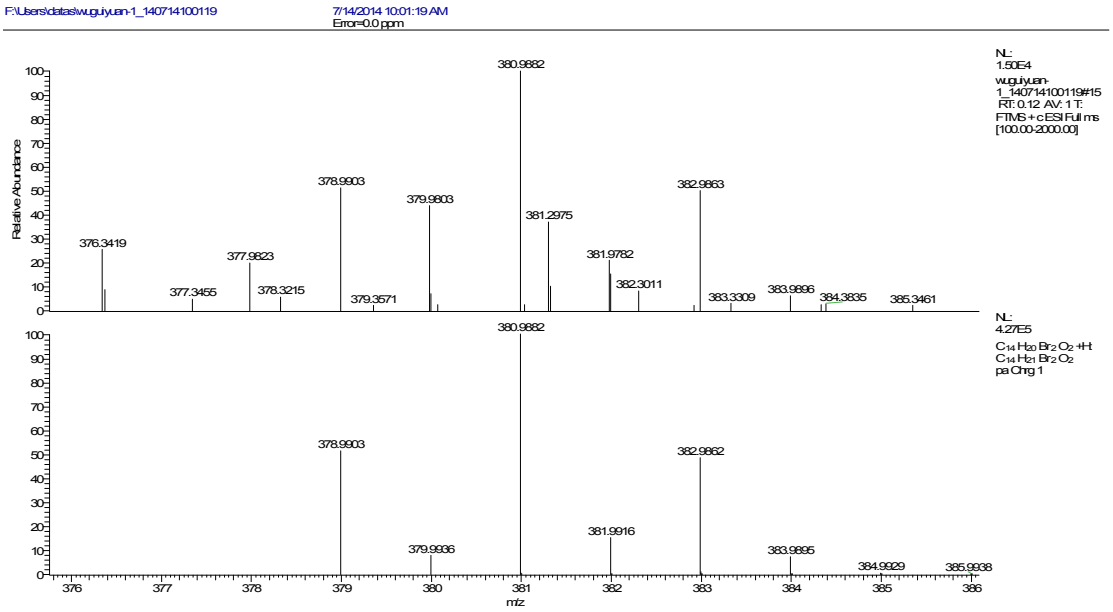

Fig. S3. High resolution electrospray ionization mass spectrum of 1.

Synthesis of 2

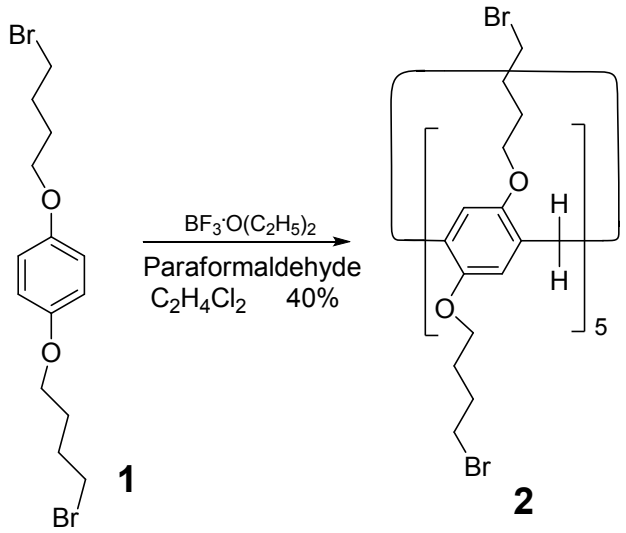

A solution of 1 (3.8 g, 10.0 mmol) in 1, 2-dichloroethane (200 mL), paraformaldehyde (0.686 g, 20.0 mmol) was added under nitrogen atmosphere. Then boron trifluoride diethyl etherate ($BF_3 \cdot O(C_2H_5)_2$, 1.42 g, 10.0 mmol) was added to the solution and the mixture was stirred at room temperature for 4 h. A green solution was obtained. After the solvent was removed, the obtained solid was purified by column chromatography on silica gel with petroleum ether/dichloromethane (1:1 v/v) as the eluent to get a white powder (1.57 g, 40 %). m.p. 124-126 °C. The ^{1}H NMR spectrum of 2 is shown in Fig.S4. ^{1}H NMR (400 MHz, $CDCl_3$) δ(ppm): 6.82 (s, 10H), 3.94 (s, 20H), 3.75 (s, 10H), 3.45 (s, 10H), 3.25 (s, 10H), 2.00 (d, J = 47.7 Hz, 41H). The ^{13}C NMR spectrum of 2 is shown in Fig. S5. ^{13}C NMR (100 MHz, $CDCl_3$) δ (ppm): 149.79, 128.33, 114.77, 67.58, 67.44, 33.74, 31.12, 30.27 and 29.70. HRESIMS is shown in Fig S6: m/z calcd for $[M + 6H]^+$ $C_{75}H_{100}Br_{10}O_{10}$, m/z 1965.92 ; found 1966.9.

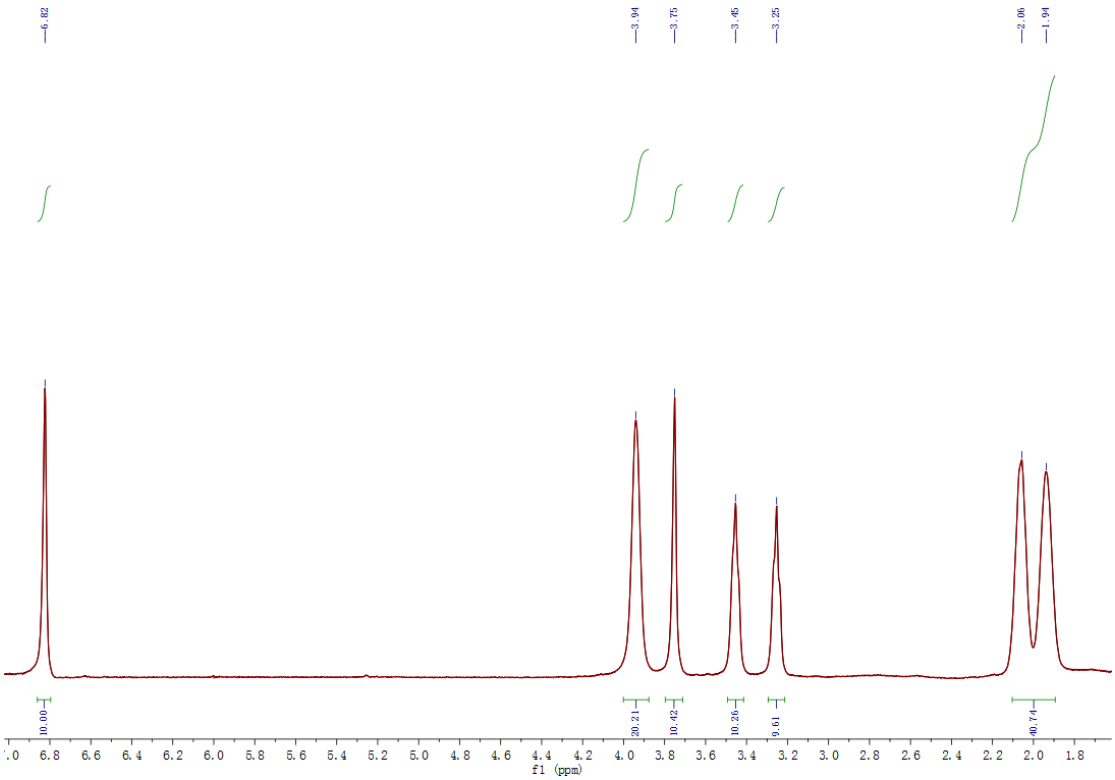

Fig. S4. ^{1}H NMR (400MHz) spectra of product 2 in $CDCl_3$.

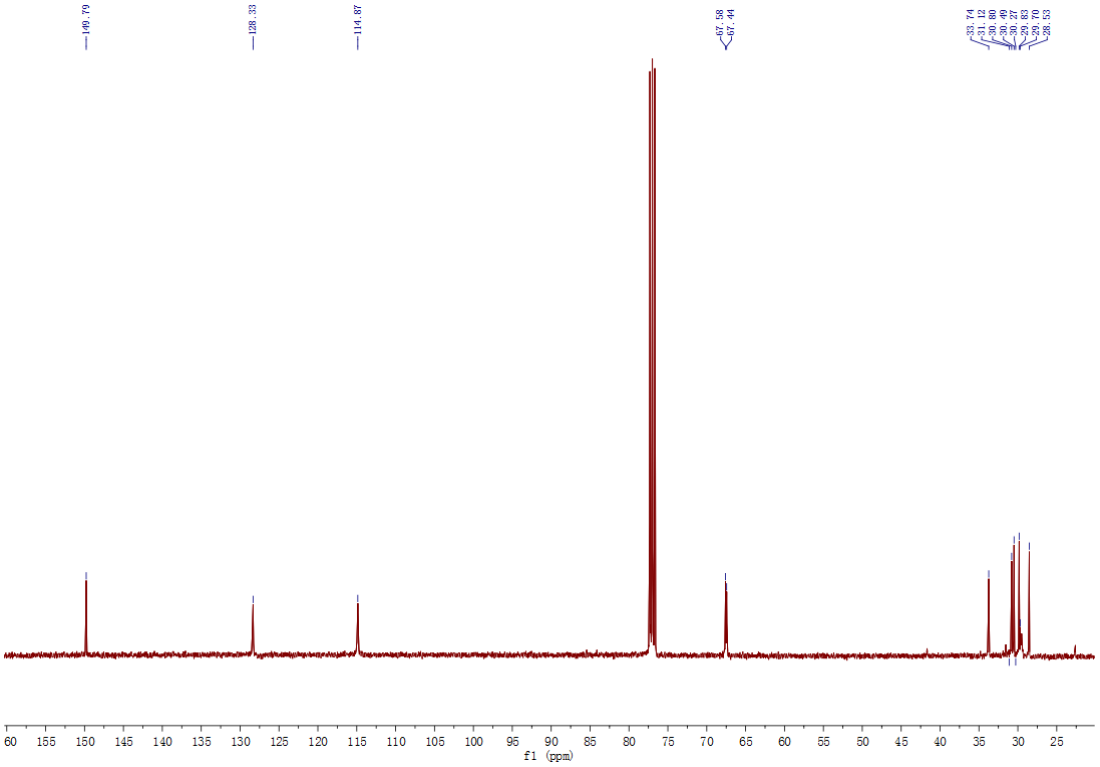

Fig. S5. ^{13}C NMR (400MHz, 298K) spectra of product 2 in $CDCl_3$.

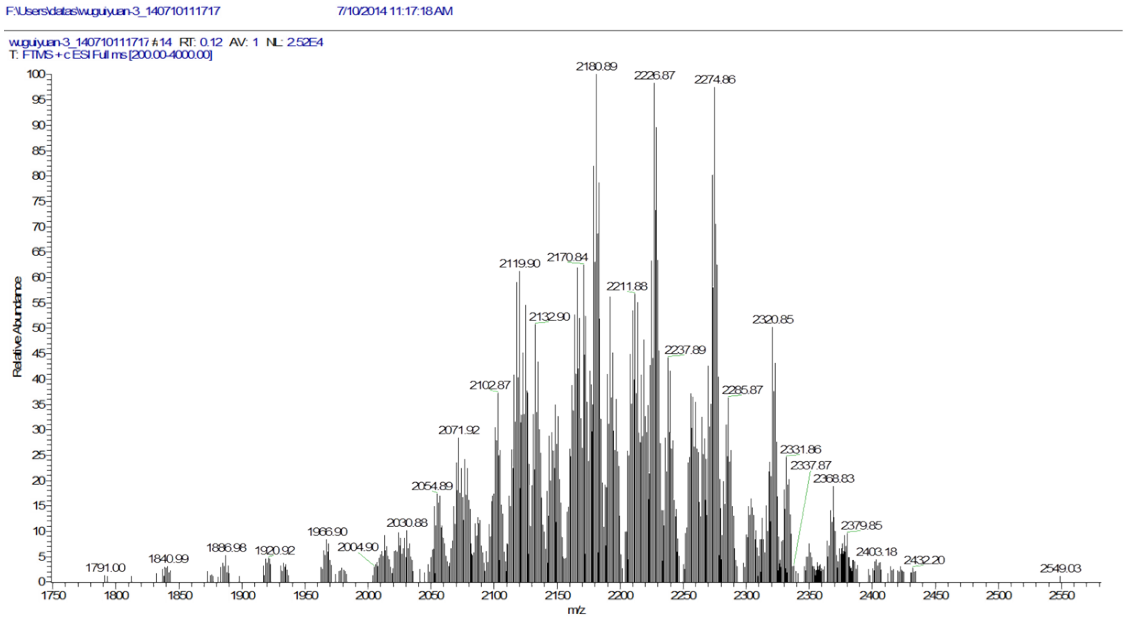

Fig. S6. High resolution electrospray ionization mass spectrum of 2.

Synthesis of compound P

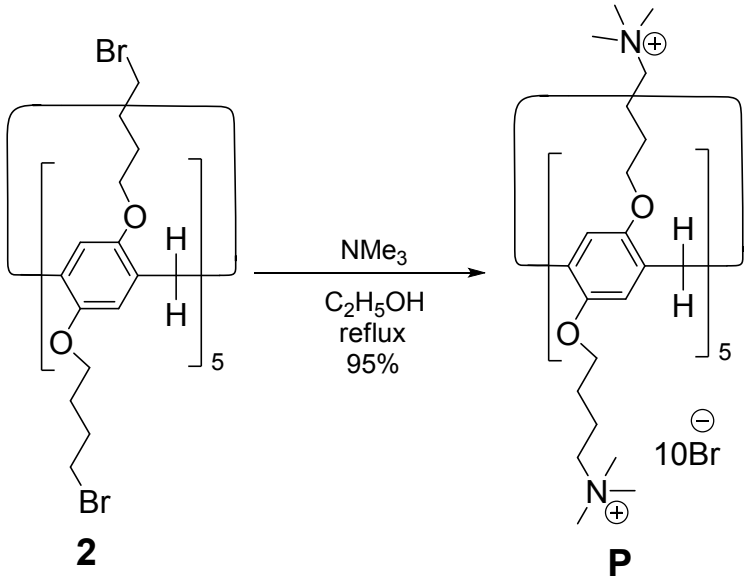

Compound 2 (1.00 g, 0.51 mmol) and trimethylamine (33 % in ethanol, 6.89 mL, 25.5 mmol) were added to ethanol (50 mL). The solution was refluxed overnight. Then the solvent was removed by evaporation, deionized water (20 mL) was added. After filtration, a clear solution was obtained. Then the water was removed by evaporation to obtain **P** as a colorless solid (1.28 g, 95 %). m.p. 218-220 °C. The ^{1}H NMR spectrum of **P** is shown in Fig. S7. ^{1}H NMR (400 MHz, D_2O) δ (ppm): 6.73 (s, 10H), 3.79 (s, 31H), 3.09 (s, 21H), 2.90 (s, 93H), 1.54 (s, 41H). The ^{13}C NMR spectrum of **P** is shown in Fig. S7. ^{13}C NMR (100 MHz, D_2O) δ (ppm): 152.86, 132.00, 71.48, 68.79, 28.49 and 22.18. HRESIMS is shown in Fig. S9: m/z of $C_{85}H_{150}Br_{10}N_{10}O_{10}$ 772.3, 557.75, 433.97 and 349.70, 288.47 corresponding to $[M-3Br]^{3+}$, $[M-4Br]^{4+}$, $[M-5Br+Na^{+}]^{5+}$, $[M-6Br+Na^{+}]^{6+}$ and $[M-7Br+Na^{+}]^{7+}$.

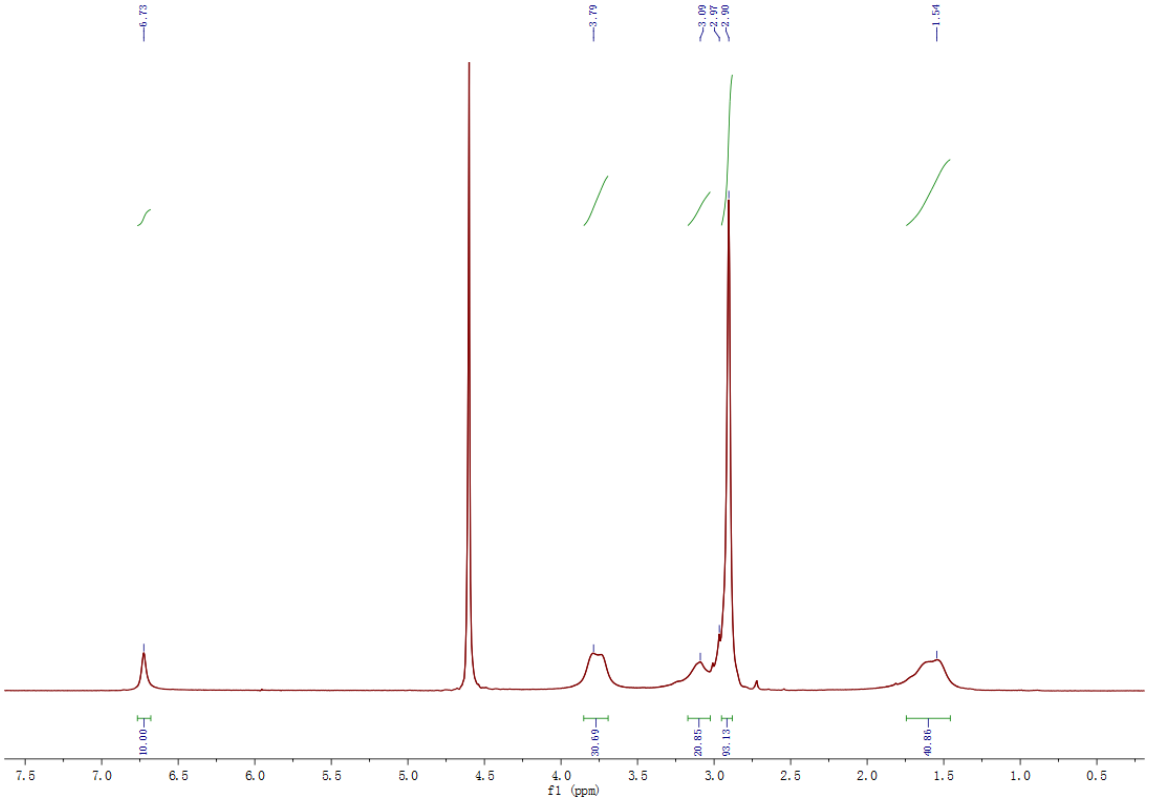

Fig. S7. ^{1}H NMR (400MHz, 298K) spectra of product **P** in D_2O.

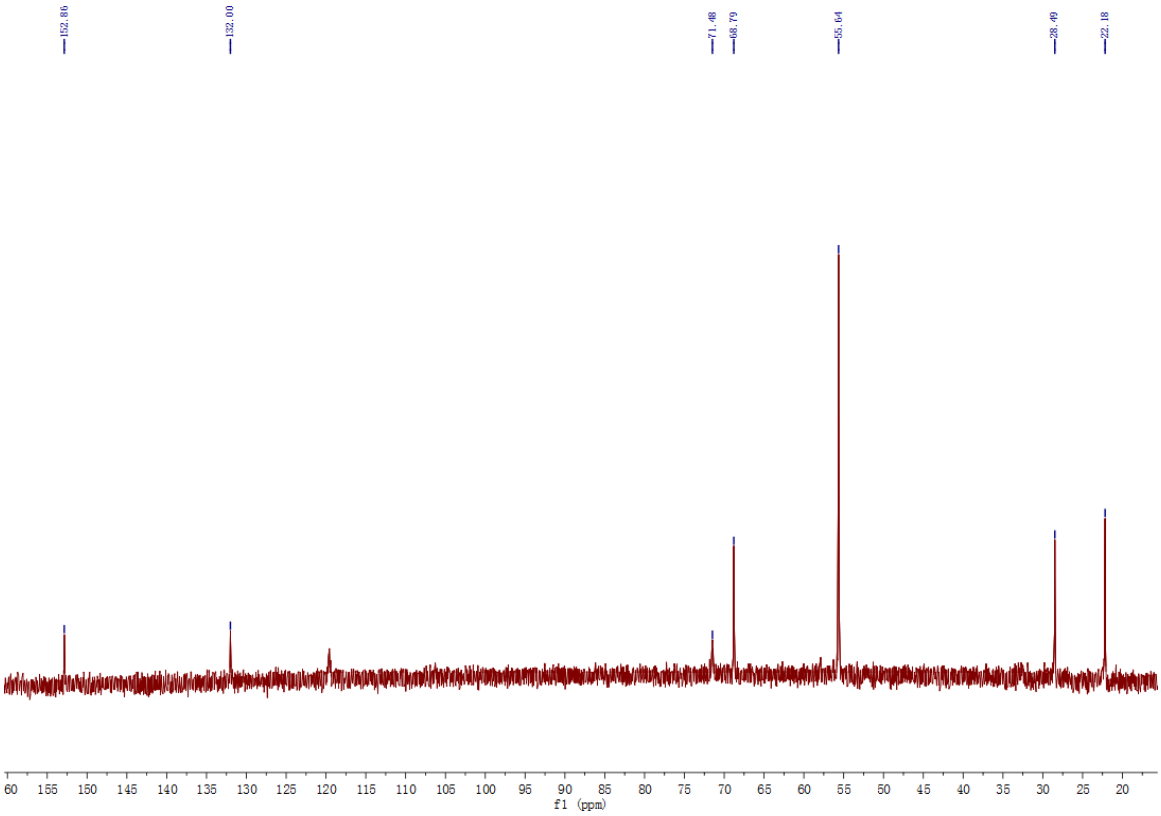

Fig. S8. ^{13}C NMR (400MHz, 298K) spectra of product **P** in D_2O.

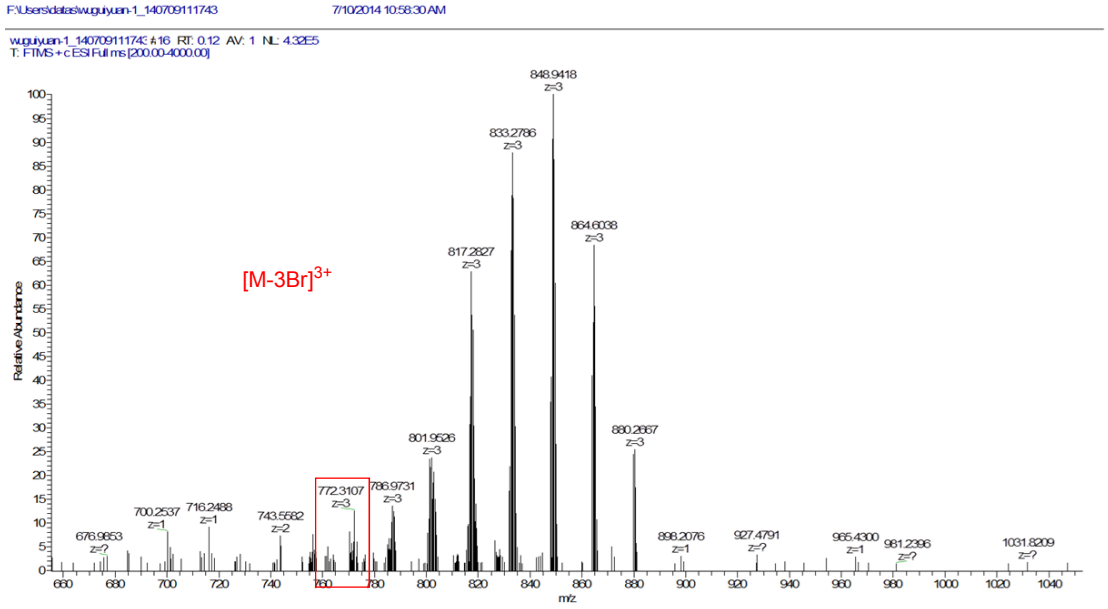
F:\Users\datas\wuguiyuan-1_140709111743 7/10/2014 10:58:30 AM
wuguiyuan-1_140709111743 #16 RT: 0.12 AV: 1 NL: 4.32E5
T: FTMS + c ESI Full ms [200.00-4000.00]
[M-3Br]3+
848.9418 z=3
833.2786 z=3
864.6038 z=3
817.2827 z=3
880.2867 z=3
801.9526 z=3
772.3107 z=3
786.9731 z=3
700.2537 z=1
716.2488 z=1
743.5582 z=2
676.9853 z=?
898.2076 z=1
927.4791 z=?
965.4300 z=1
981.2396 z=?
1031.8209 z=?
Relative Abundance
m/z

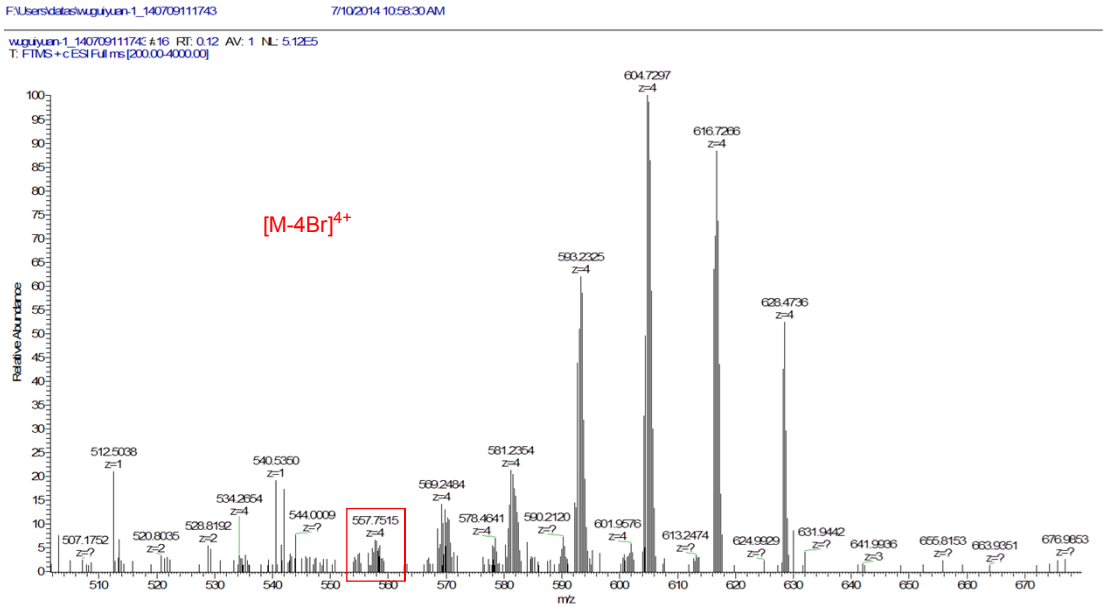
F:\Users\datas\wuguiyuan-1_140709111743 7/10/2014 10:58:30 AM
wuguiyuan-1_140709111743 #16 RT: 0.12 AV: 1 NL: 5.12E5
T: FTMS + c ESI Full ms [200.00-4000.00]
[M-4Br]4+
604.7297 z=4
616.7286 z=4
593.2325 z=4
628.4736 z=4
581.2354 z=4
569.2484 z=4
512.5038 z=1
540.5350 z=1
534.2654 z=4
544.0009 z=?
557.7515 z=4
578.4641 z=4
590.2120 z=?
601.9576 z=4
613.2474 z=?
624.9929 z=?
631.9442 z=?
641.9936 z=3
655.8153 z=?
663.9351 z=?
676.9853 z=?
507.1752 z=?
520.8035 z=2
528.8192 z=2
Relative Abundance
m/z

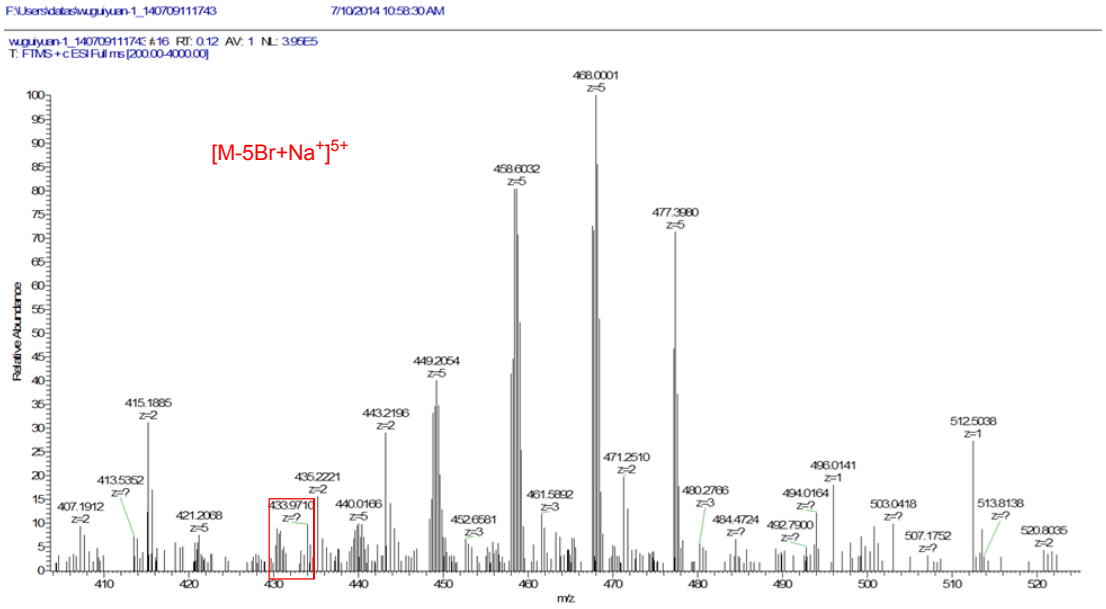
F:\Users\datas\wuguiyuan-1_140709111743 7/10/2014 10:58:30 AM
wuguiyuan-1_140709111743 #16 RT: 0.12 AV: 1 NL: 3.95E5
T: FTMS + c ESI Full ms [200.00-4000.00]
[M-5Br+Na+]5+
Relative Abundance
m/z

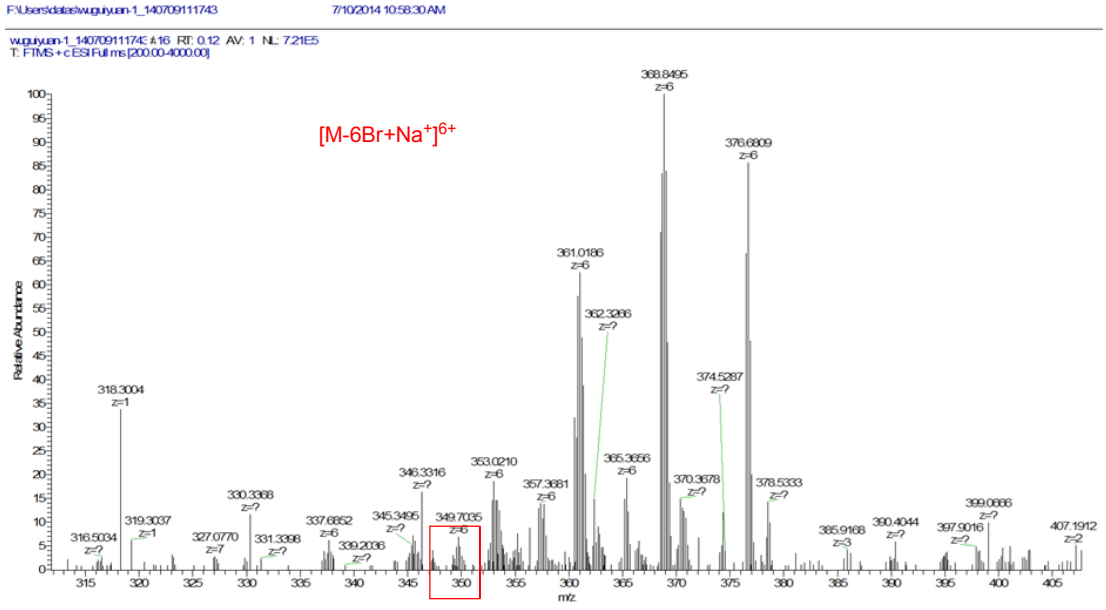
F:\Users\datas\wuguiyuan-1_140709111743 7/10/2014 10:58:30 AM
wuguiyuan-1_140709111743 #16 RT: 0.12 AV: 1 NL: 7.21E5
T: FTMS + c ESI Full ms [200.00-4000.00]
[M-6Br+Na+]6+
Relative Abundance
m/z

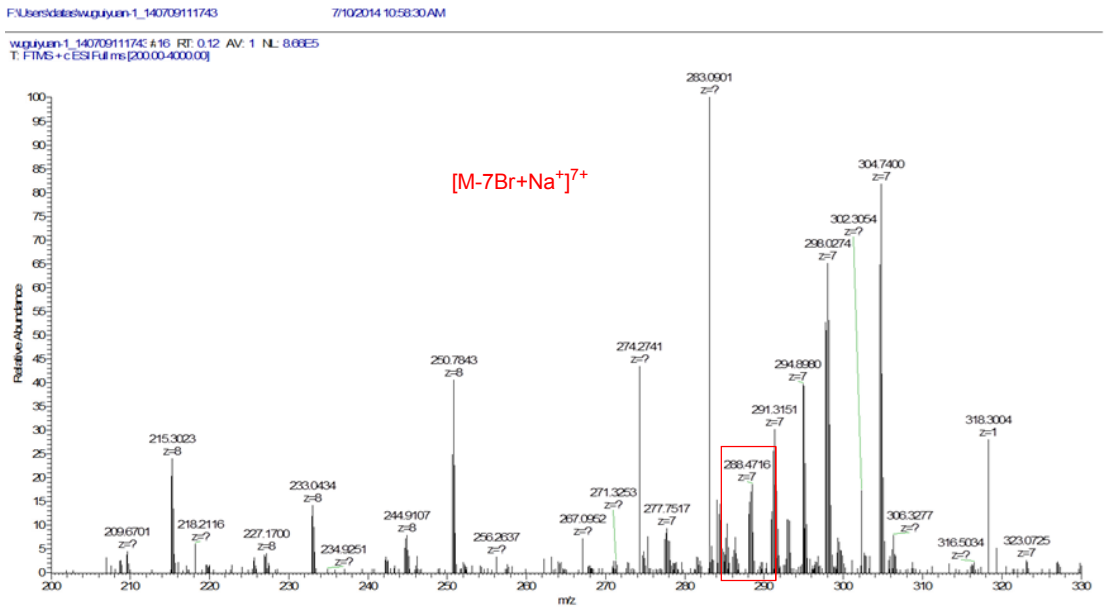

Fig. S9. High resolution electrospray ionization mass spectrum of **P**.

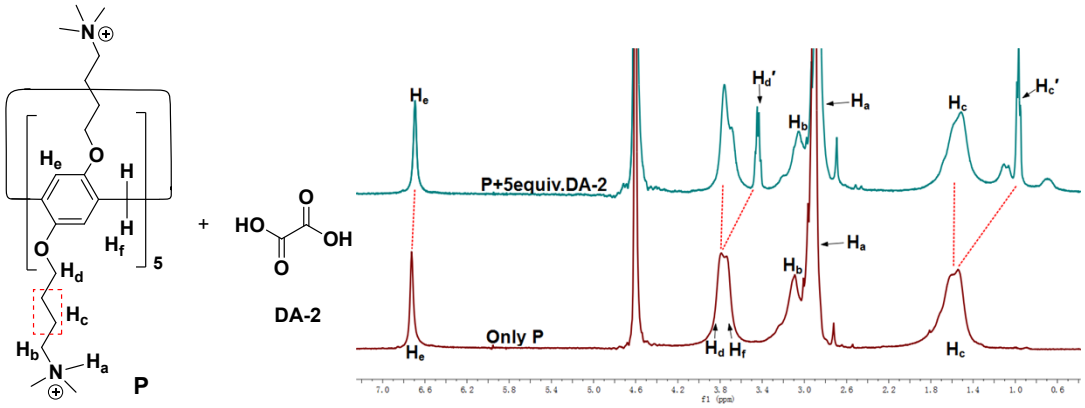

Fig. S10. ^{1}H NMR spectra (400MHz, 298K) of **P** (10 mM) with DA-2 (50mM) in D_2O.

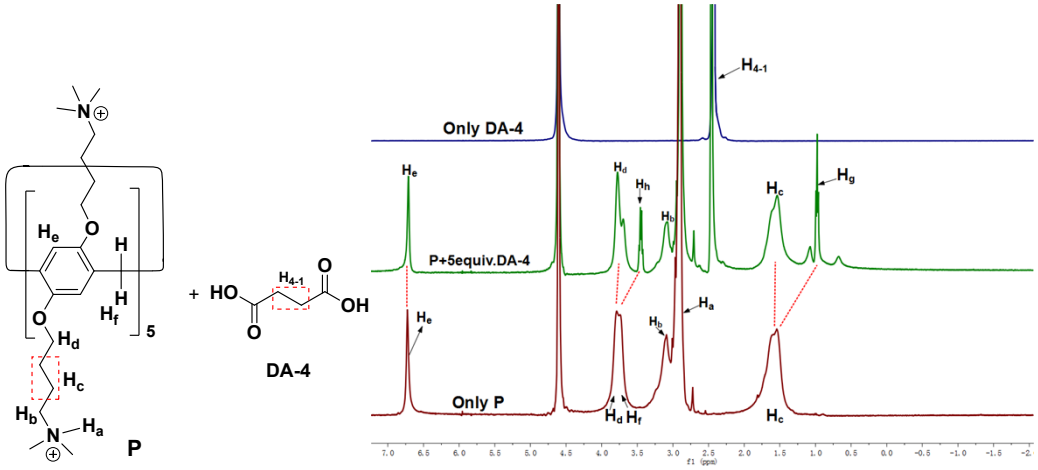

Fig. S11. ^{1}H NMR spectra (400MHz, 298K) of **P** (10.0 mM) with DA-4 (50.0mM) in D_2O.

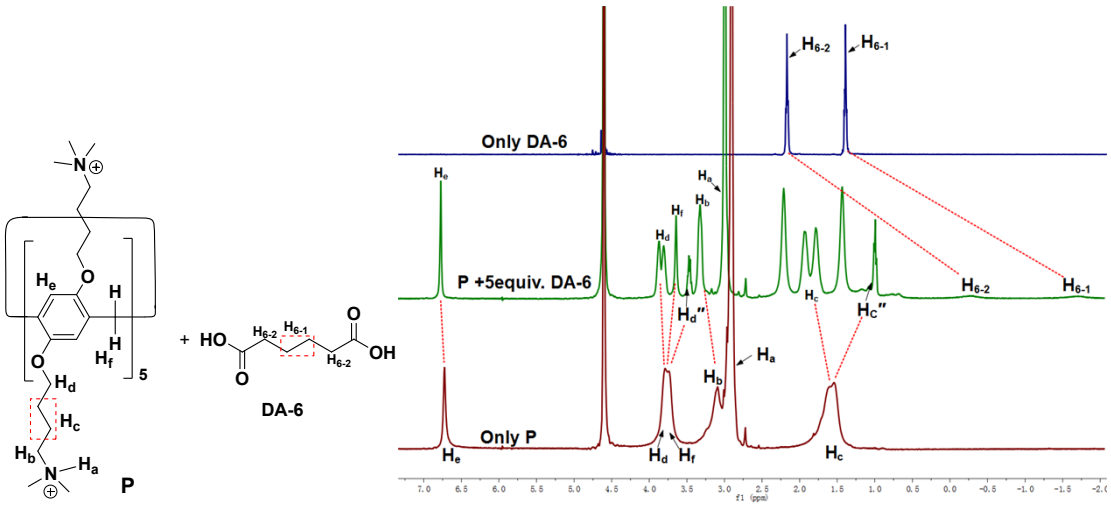

Fig S12. ^{1}H NMR spectra (400MHz, 298K) of **P** (10.0 mM) with DA-6 (50.0 mM) in D_2O.

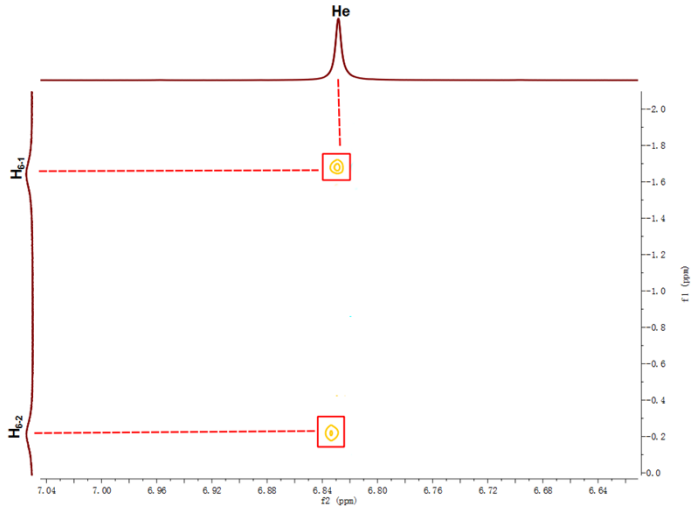

Fig. S13. ^{1}H NOESY NMR spectra (600 MHz) of the complex of **P** (15.0 mM) with DA-6 in a 1:2 molar ratio (30.0 mM) in D_2O at ambient temperature.

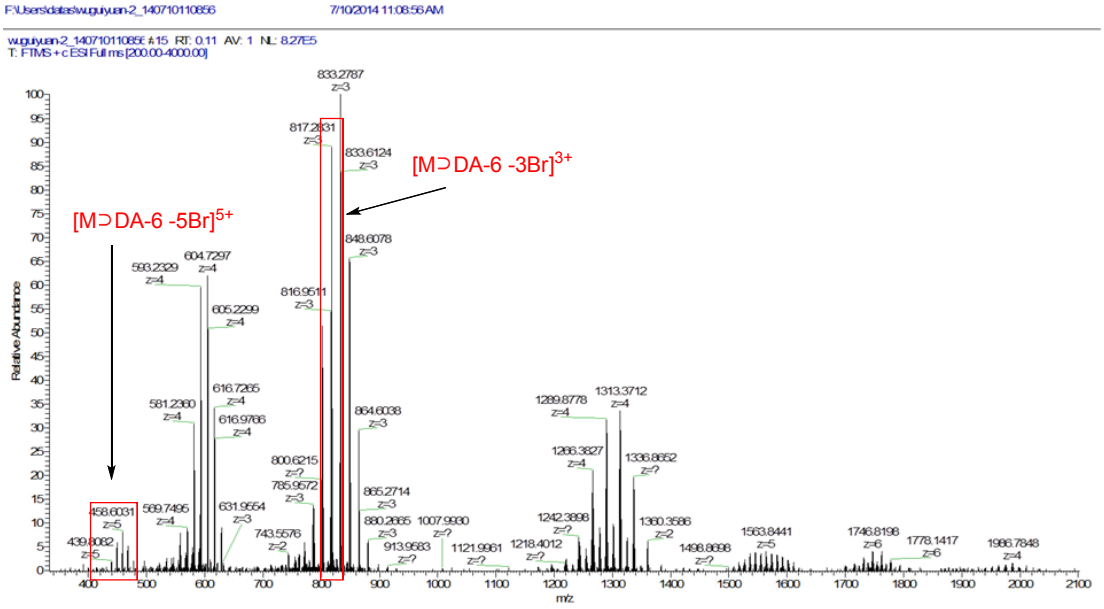

Fig. S14. Electrospray ionization mass spectrum of the complex of **P** with DA-6 (30.0 mM) in a 1:2 molar ratio. Assignment of main peaks: m/z 458.6 $[H\supset DA\text{-}6 - 5Br]^{5+}$, 817.28 $[H\supset DA\text{-}6 - 3Br]^{3+}$.

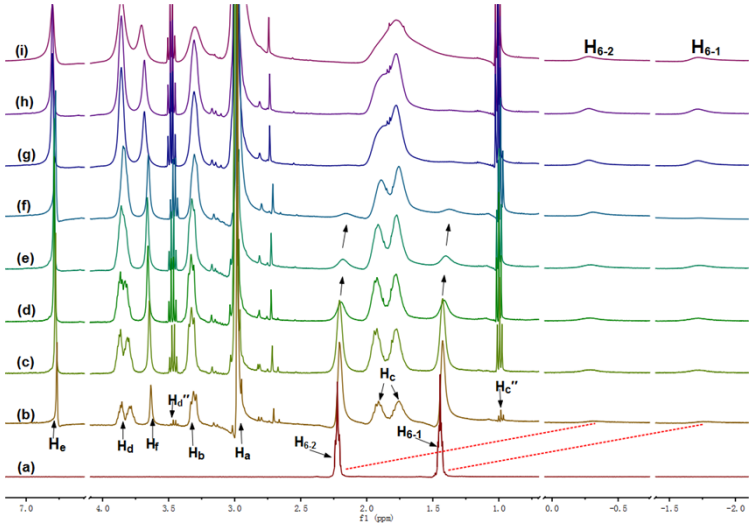

Fig. S15. Partial ^{1}H NMR spectra of DA-6 (15.0 mM, D_2O, 400 MHz) and in the presence of varying amounts of **P**. The mole ratio of **P** to DA-6 is (a) 0, (b) 0.2, (c) 0.4, (d) 0.6, (e) 0.8, (f) 1.0, (g) 1.5, (h) 2.0, (i) 3.0, respectively.

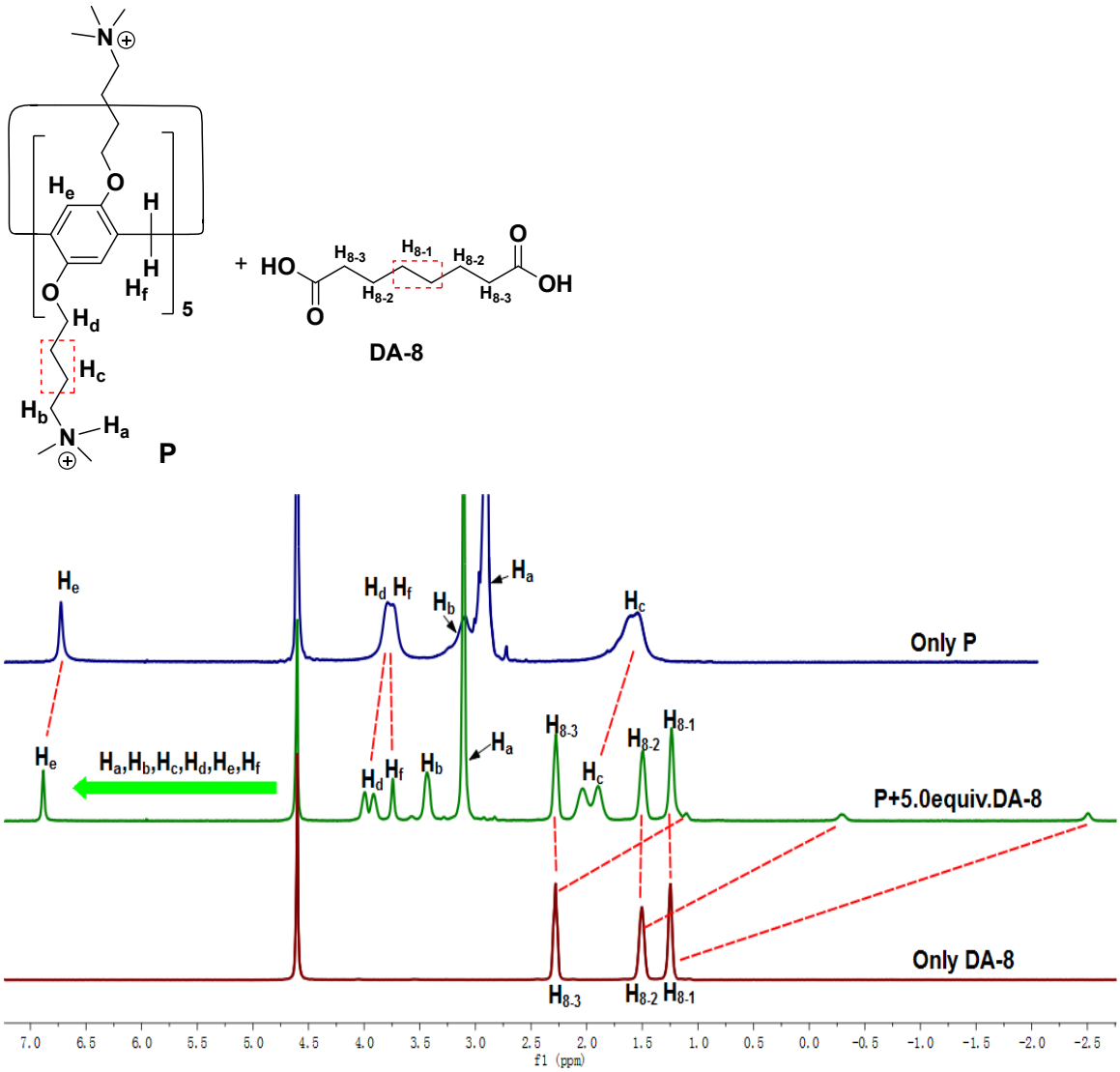

Fig S16. ^{1}H NMR spectra (400MHz, 298K) of **P** (10.0 mM) with DA-8 (50.0 mM) in D_2O.

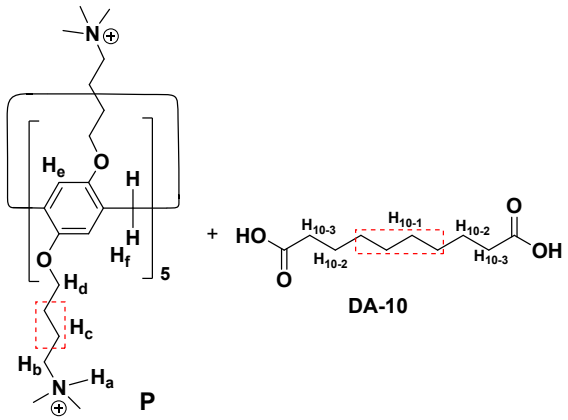

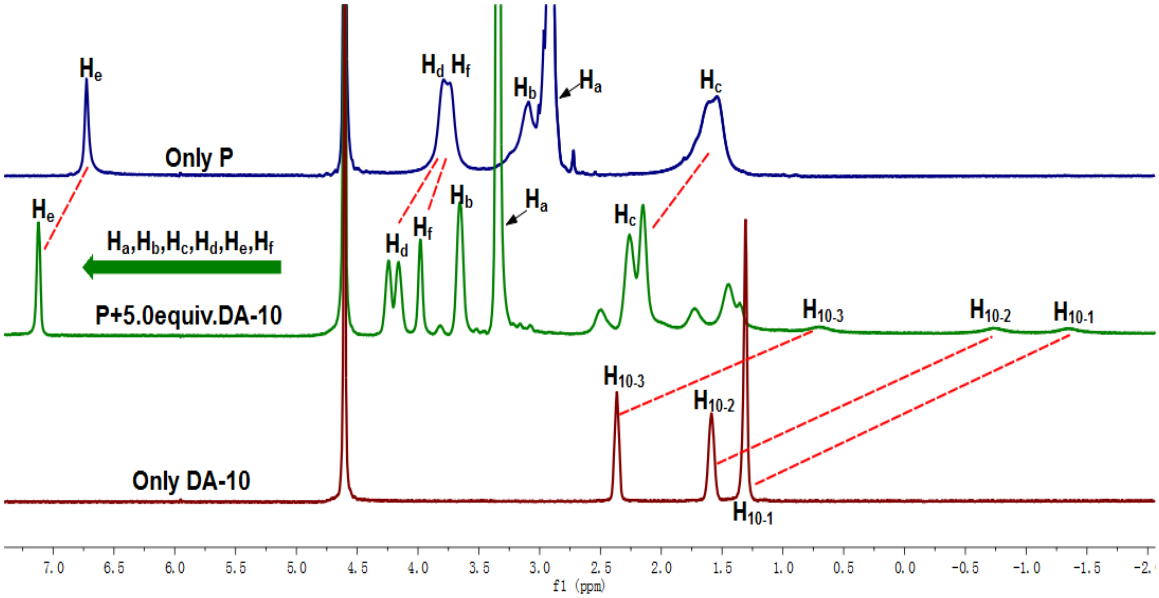

Fig S17. ^{1}H NMR spectra (400MHz, 298K) of **P** (10.0 mM) with DA-10 (50.0 mM) in D_2O.

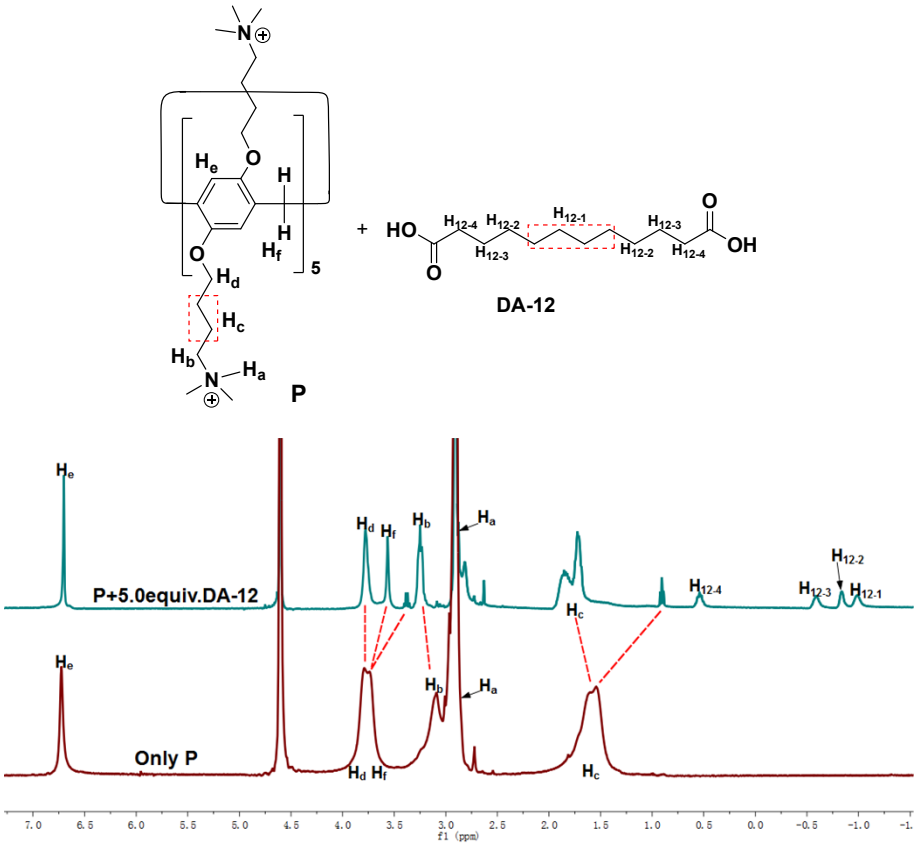

Fig S18. ^{1}H NMR spectra (400MHz, 298K) of **P** (10.0 mM) with DA-12 (50.0 mM) in D_2O.

Table S1. Chemical shifts (δ) and chemical shift changes (Δδ) of hydrogen on free **P**

and encapsulated DA-n. Δδ (=$\delta_{encapsulated} - \delta_{free}$, ppm)

Diacids	H_a(Δδ, ppm)	H_b(Δδ, ppm)	H_e(Δδ, ppm)	H_f(δ, ppm)
P	2.904	3.09	6.724	—
P+DA-2	-0.034	-0.037	-0.032	—
P+DA-4	-0.011	-0.008	-0.013	—
P+DA-6	0.088	0.231	0.049	3.624
P+DA-8	0.202	0.344	0.16	3.742
P+DA-10	0.337	0.565	0.398	3.98
P+DA-12	0.004	0.159	-0.023	3.582

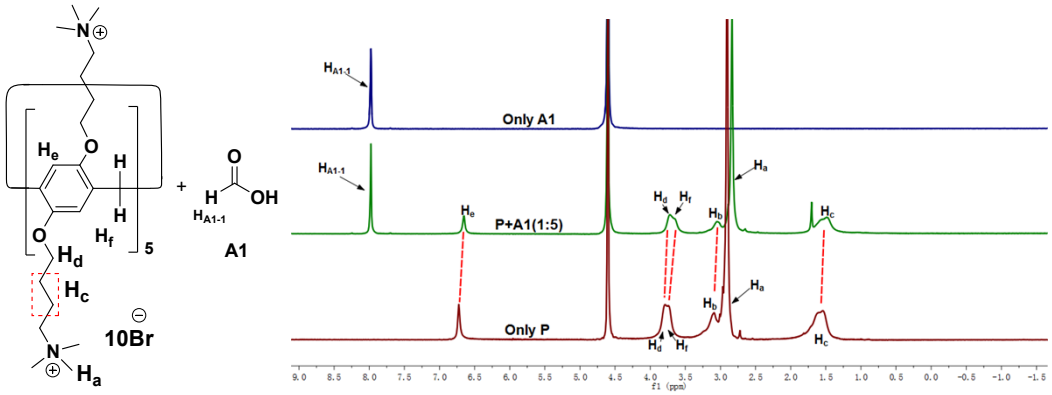

Fig S19. ^{1}H NMR spectra (400MHz, 298K) of **P** (10.0 mM) with A1 (50.0 mM) in D_2O.

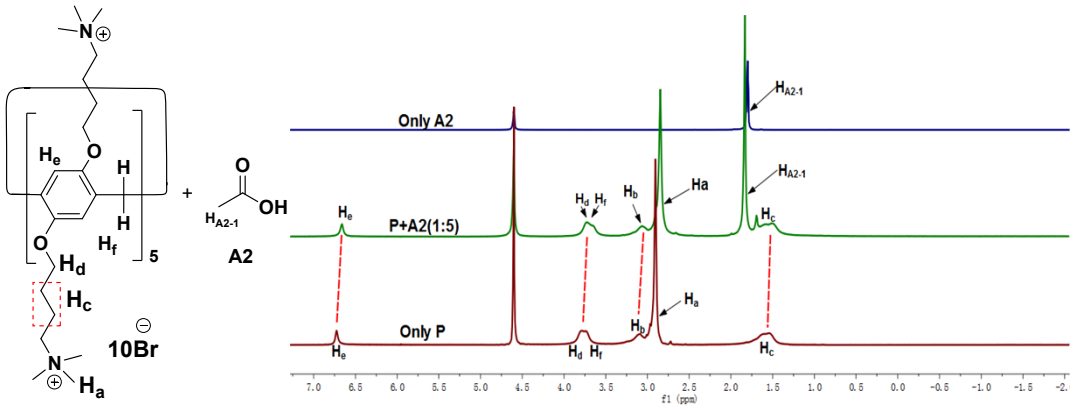

Fig S20. ^{1}H NMR spectra (400MHz, 298K) of **P** (10.0 mM) with A2 (50.0 mM) in D_2O.

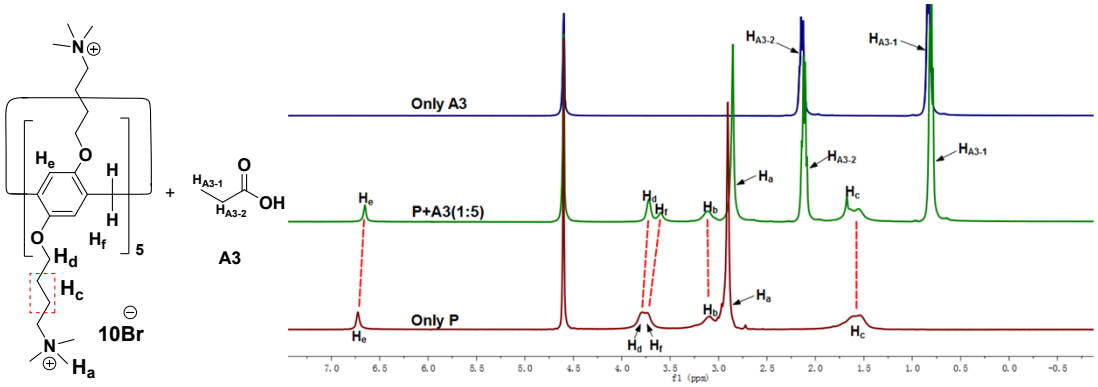

Fig S21. ^{1}H NMR spectra (400MHz, 298K) of **P** (10.0 mM) with A3 (50.0 mM) in D_2O.

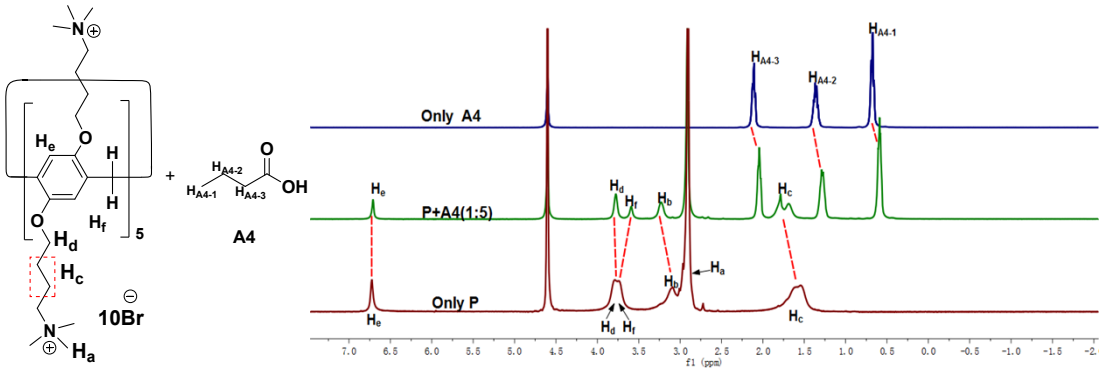

Fig S22. ^{1}H NMR spectra (400MHz, 298K) of **P** (10.0 mM) with A4 (50.0 mM) in D_2O.

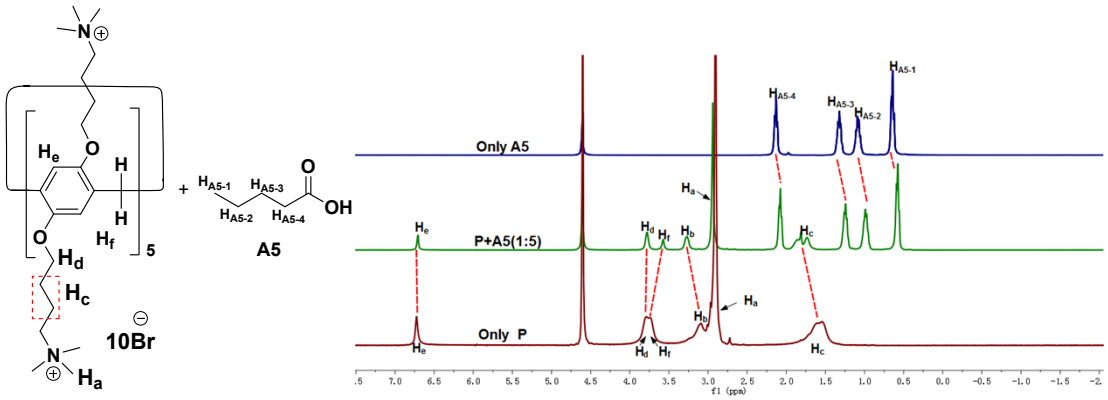

Fig S23. ^{1}H NMR spectra (400MHz, 298K) of **P** (10.0 mM) with A5 (50.0 mM) in D_2O.

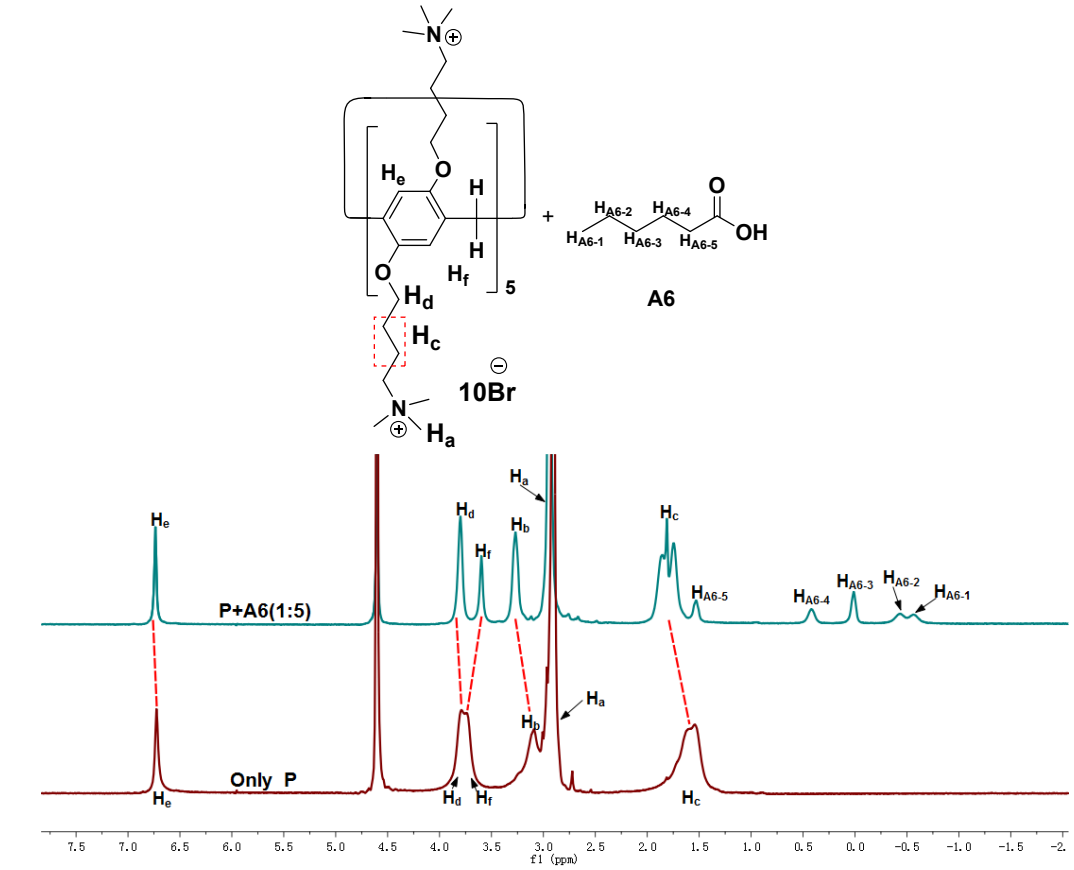

Fig S24. ^{1}H NMR spectra (400MHz, 298K) of **P** (10.0 mM) with A6 (50.0 mM) in D_2O.

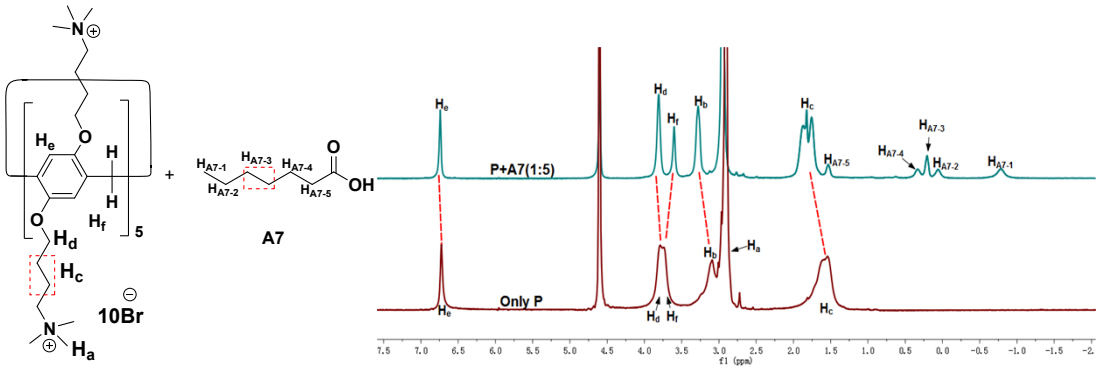

Fig S25. ^{1}H NMR spectra (400MHz, 298K) of **P** (10.0 mM) with A7 (50.0 mM) in D_2O.

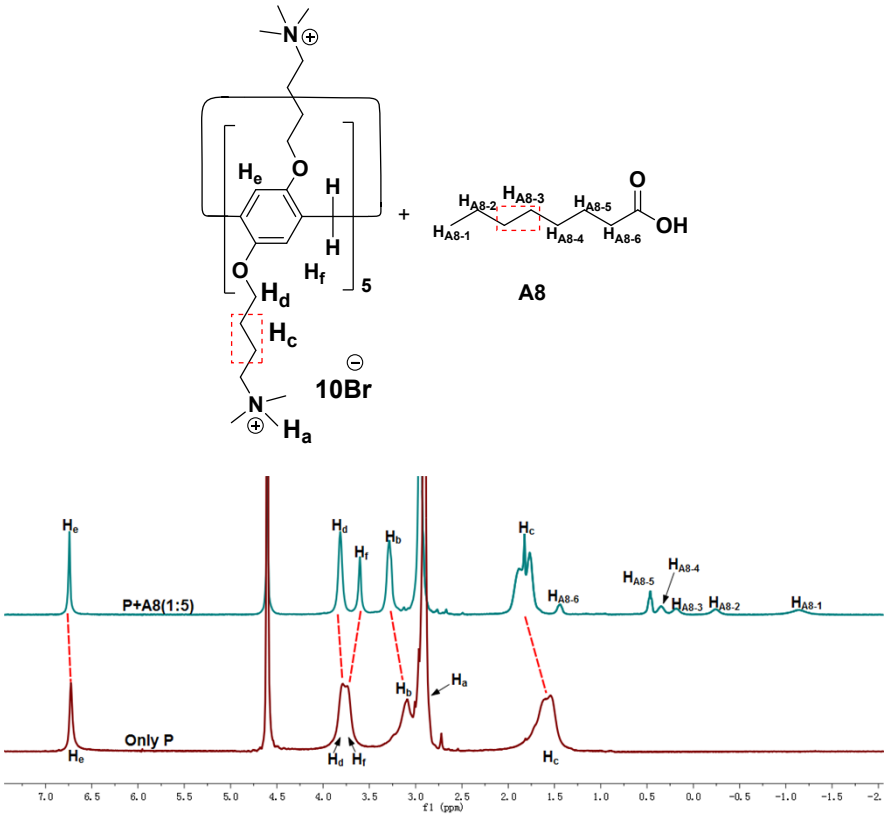

Fig S26. ^{1}H NMR spectra (400MHz, 298K) of **P** (10.0 mM) with A8 (50.0 mM) in D_2O.

Table S2. Chemical shifts (δ) and chemical shift changes (Δδ) of hydrogen on free **P** and encapsulated A-n. Δδ (=$\delta_{encapsulated} - \delta_{free}$, ppm)

	H_a(Δδ, ppm)	H_b(Δδ, ppm)	H_d(δ, ppm)	H_e(Δδ, ppm)	H_f(δ, ppm)
P	2.904	3.09	—	6.724	—
P+A1	-0.072	-0.041	—	-0.071	—
P+A2	-0.056	-0.027	—	-0.063	—
P+A3	-0.051	0.019	3.719	-0.073	3.596
P+A4	-0.009	0.135	3.775	-0.014	3.59
P+A5	0.033	0.18	3.778	-0.017	3.573
P+A6	0.043	0.197	3.792	-0.004	3.576
P+A7	0.044	0.194	3.805	0.008	3.59
P+A8	0.042	0.193	3.809	0.013	3.596

Table S3. Chemical shifts (δ) and chemical shift changes (Δδ) of hydrogen on free **P** and encapsulated DA-n with CF_3COOH. Δδ (=$\delta_{encapsulated\ with\ CF3COOH} - \delta_{encapsulated}$, ppm)

Diacids (n)	δ of CH_2 on encapsulated diacids ($\delta_{encapsulated}$, ppm)				δ of CH_2 on encapsulated diacids with CF_3COOH				Δδ(=$\delta_{encapsulated\ with\ CF3COOH} - \delta_{encapsulated}$, ppm)			
	H1	H2	H3	H4	H1	H2	H3	H4	H1	H2	H3	H4
DA-6	-1.687	-0.278	—	—	-2.174	-0.696		—	-0.487	-0.418	—	—
DA-8	-2.508	-0.301	1.102	—	-2.962	-0.744	1.033	—	-0.454	-0.443	-0.069	—
DA-10	-1.354	-0.743	0.705	—	-2.392	-1.699	-0.243	—	-1.038	-0.956	-0.948	—
DA-12	-0.985	-0.838	-0.585	0.541	-1.363	-1.29	-0.902	0.205	-0.378	-0.452	-0.317	-0.336

Table S4. Chemical shifts (δ) and chemical shift changes (Δδ) of hydrogen on free P and encapsulated A-n with F_3CCOOH. Δδ (=$\delta_{encapsulated\ with\ F3CCOOH} - \delta_{encapsulated}$, ppm)

Acids(n)	δ of CH_2 on encapsulated diacids ($\delta_{encapsulated}$, ppm)						δ of CH_2 on encapsulated diacids with CF_3COOH						Δδ(=$\delta_{encapsulated\ with\ TEA} - \delta_{encapsulated}$, ppm)					
	H1	H2	H3	H4	H5	H6	H1	H2	H3	H4	H5	H6	H1	H2	H3	H4	H5	H6
A3	0.801	2.122	□	□	□	□	0.448	1.764	□	□	□	□	-0.353	-0.358	□	□	□	□
A4	0.593	1.287	2.047	□	□	□	0.449	1.147	1.903	□	□	□	-0.144	-0.14	-0.144	□	□	□
A5	0.573	0.99	1.242	2.074	□	□	0.211	0.607	0.895	1.729	□	□	-0.362	-0.383	-0.345	□	□	□
A6	-0.569	-0.424	0.012	0.421	1.537	□	-0.539	-0.433	-0.008	0.452	1.549	□	0.03	-0.009	-0.02	0.031	0.012	□
A7	-0.782	0.061	0.207	0.333	1.535	□	-0.913	-0.049	0.131	0.288	1.488	□	-0.131	-0.11	-0.076	-0.045	-0.047	□
A8	-1.136	-0.231	0.185	0.354	0.464	1.447	-1.144	-0.306	0.199	0.286	0.393	1.421	-0.008	-0.075	0.14	-0.068	-0.071	-0.026

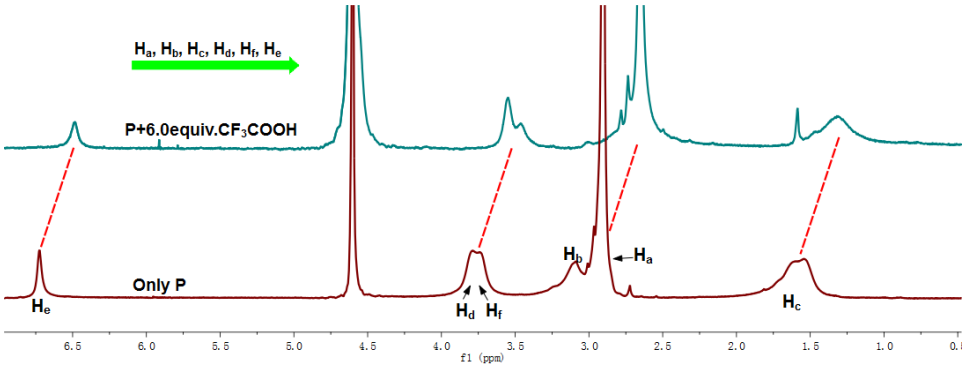

Fig S27. ^{1}H NMR spectra (400MHz, 298K) of P (10.0 mM) with CF_3COOH (60.0 mM) in D_2O.

Table S5. Chemical shifts (δ) and chemical shift changes (Δδ) of hydrogen on free **P** and encapsulated DA-n with TEA. Δδ (=$\delta_{\text{encapsulated with TEA}} - \delta_{\text{encapsulated}}$, ppm)

Diacids (n)	δ of CH_2 on encapsulated diacids ($\delta_{\text{encapsulated}}$, ppm)				δ of CH_2 on encapsulated diacids with TEA				Δδ(=$\delta_{\text{encapsulated with TEA}} - \delta_{\text{encapsulated}}$, ppm)			
	H1	H2	H3	H4	H1	H2	H3	H4	H1	H2	H3	H4
DA-6	-1.687	-0.278	—	—	-2.182	-1.113	—	—	-0.495	-0.935	—	—
DA-8	-2.508	-0.301	1.102	—	-2.694	-0.548	—	—	-0.186	-0.247	—	—
DA-10	-1.354	-0.743	0.705	—	—	—	—	—	—	—	—	—
DA-12	-0.985	-0.838	-0.585	0.541	—	—	—	—	—	—	—	—

Table S6. Chemical shifts (δ) and chemical shift changes (Δδ) of hydrogen on free **P** and encapsulated A-n with TEA. Δδ (=$\delta_{\text{encapsulated with TEA}} - \delta_{\text{encapsulated}}$, ppm)

Acids(n)	δ of CH_2 on encapsulated diacids ($\delta_{\text{encapsulated}}$, ppm)						δ of CH_2 on encapsulated diacids with TEA						Δδ(=$\delta_{\text{encapsulated with TEA}} - \delta_{\text{encapsulated}}$, ppm)					
	H1	H2	H3	H4	H5	H6	H1	H2	H3	H4	H5	H6	H1	H2	H3	H4	H5	H6
A3	0.801	2.122	□	□	□	□	0.828	2.026	□	□	□	□	0.027	-0.096	□	□	□	□
A4	0.593	1.287	2.047	□	□	□	0.582	1.27	1.902	□	□	□	-0.011	-0.017	0.154	□	□	□
A5	0.573	0.99	1.242	2.074	□	□	0.625	1.275	1.93	-	□	□	0.052	0.285	0.688	□	□	□
A6	-0.569	-0.424	0.012	0.421	1.537	□	0.351	0.694	1.14	-	-	□	0.92	1.118	1.128	□	□	□
A7	-0.782	0.061	0.207	0.333	1.535	□	0.045	0.418	1.028	-	-	□	0.827	0.357	0.821	□	□	□
A8	-1.136	-0.231	0.185	0.354	0.464	1.447	-0.705	-0.436	-0.205	-0.079	0.314	2.59	0.431	-0.205	-0.264	-0.15	1.143	□

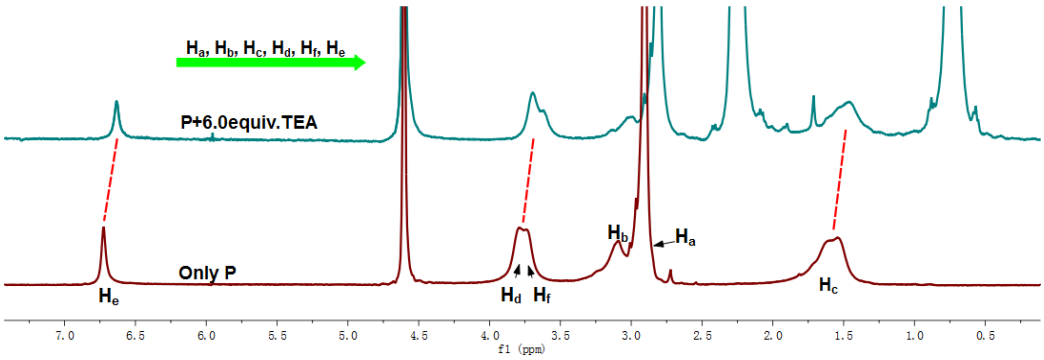

Fig S28. ^{1}H NMR spectra (400MHz, 298K) of **P** (10.0 mM) with TEA (60.0 mM) in D_2O.

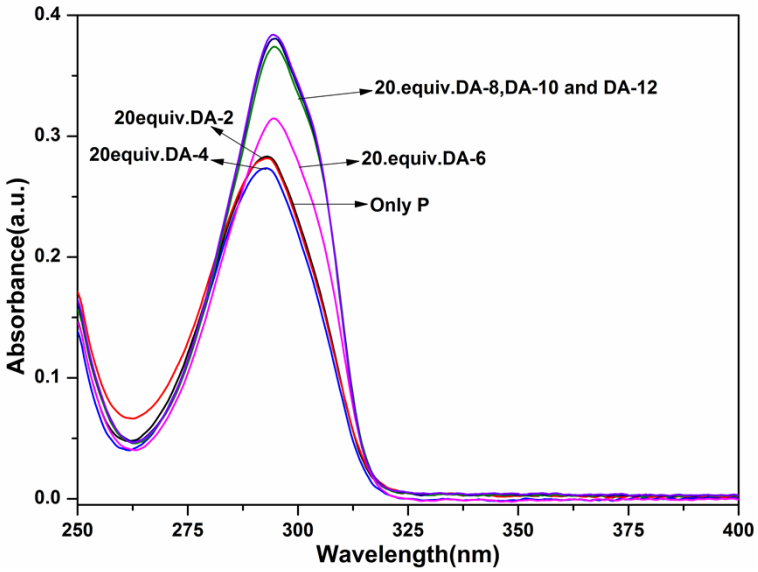

Fig. S29. UV-vis spectra change of **P** (20 μM) upon addition of 20 equiv. of DA-2, DA-4, DA-6, DA-8, DA-10 and DA-12 in H_2O (pH=7.0).

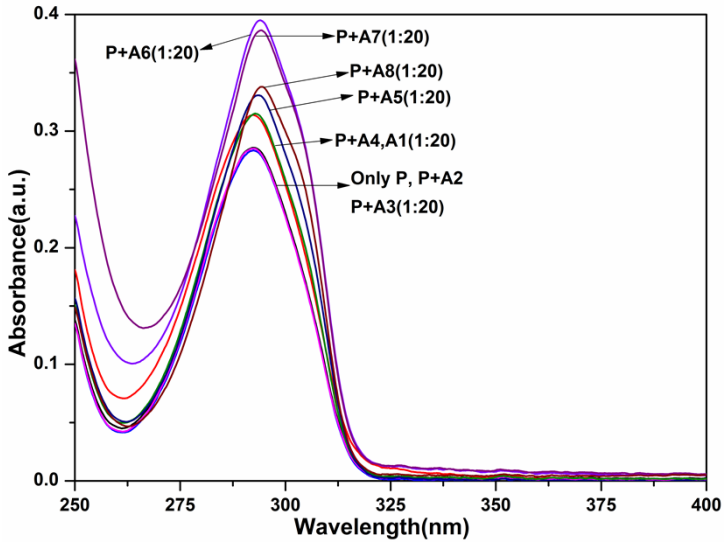

Fig. S30. UV-vis spectra change of **P** (20 μM) upon addition of 20 equiv. of A1, A2, A3, A4, A5, A6, A7 and A8 in H_2O (pH=7.0).

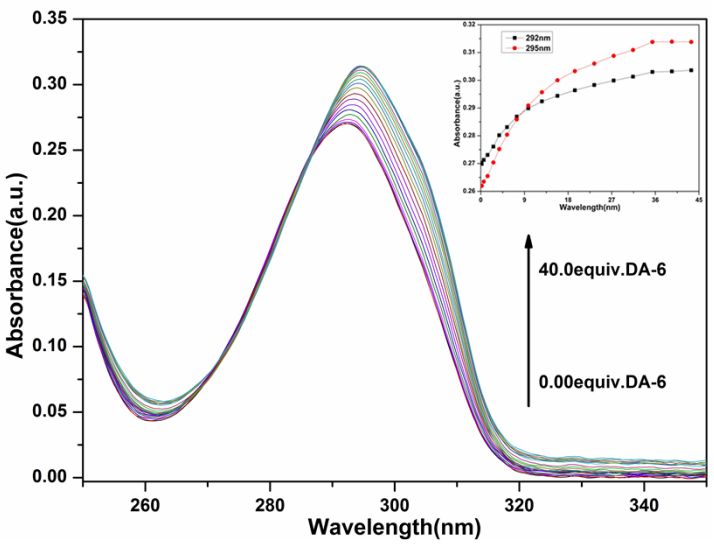

Fig. S31. UV-vis spectra of **P** (20μM) in H_2O (pH=7.0) upon adding of an increasing concentration of DA-6 from 0 to 40.0 equiv. Inset: A plot of absorption spectroscopy intensity as estimated by the peak height at 292 nm and 295 nm.

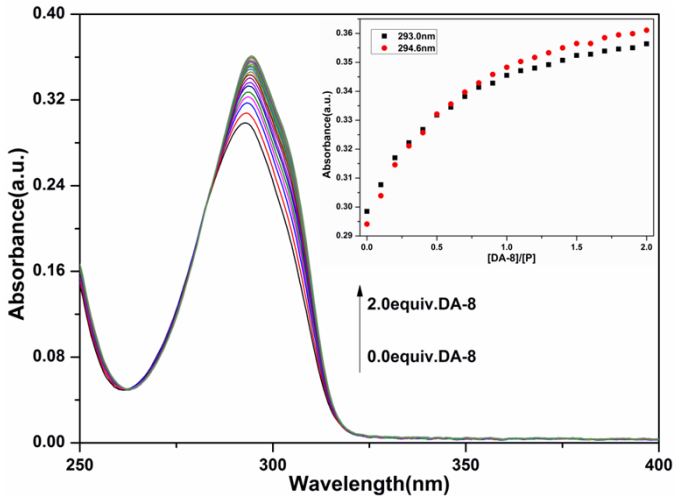

Fig. S32. UV-vis spectra of P (20μM) in H_2O (pH=7.0) upon adding of an increasing concentration of DA-8 from 0 to 2.0 equiv. Inset: A plot of absorption spectroscopy intensity as estimated by the peak height at 293 nm and 294.6 nm.

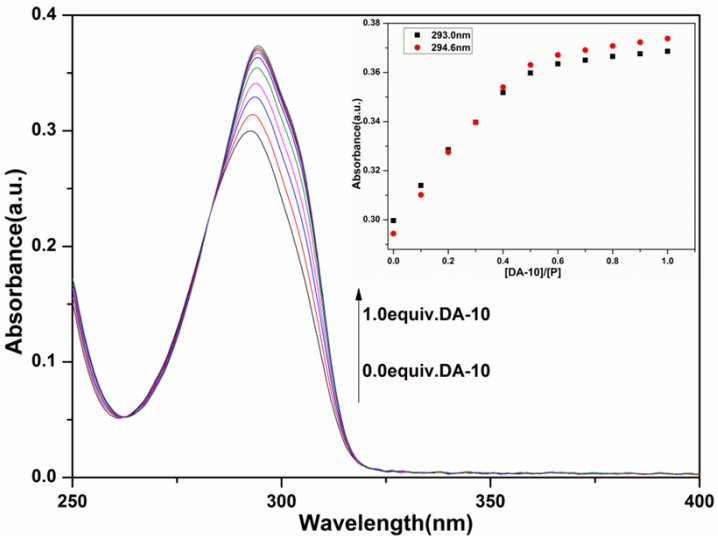

Fig. S33. UV-vis spectra of **P** (20μM) in H_2O (pH=7.0) upon adding of an increasing concentration of DA-10 from 0 to 1.0 equiv. Inset: A plot of absorption spectroscopy intensity as estimated by the peak height at 293 nm and 294.6 nm.

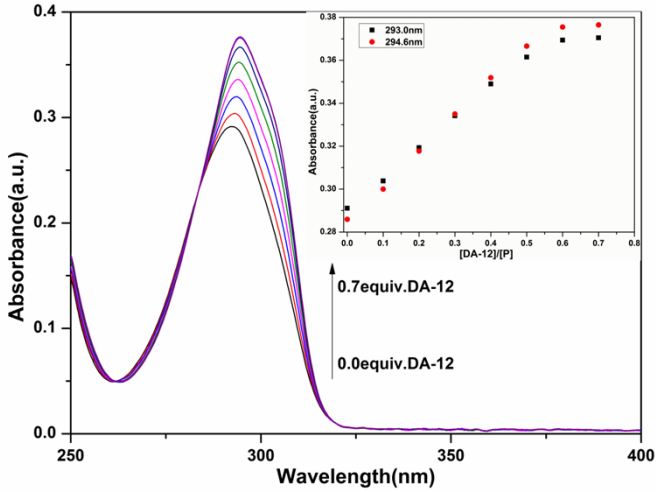

Fig. S34. UV-vis spectra of **P** (20μM) in H_2O (pH=7.0) upon adding of an increasing concentration of DA-12 from 0 to 0.7 equiv. Inset: A plot of absorption spectroscopy intensity as estimated by the peak height at 293 nm and 294.6 nm.

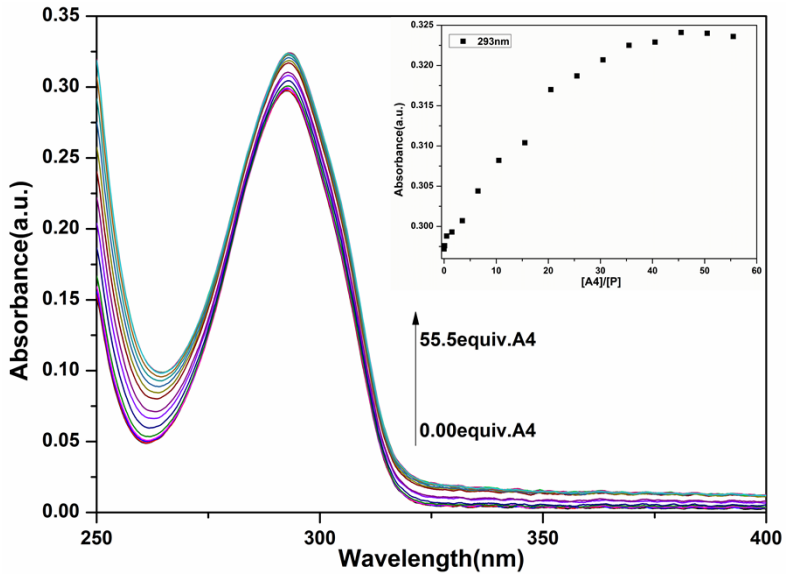

Fig. S35. UV-vis spectra of **P** (20μM) in H_2O (pH=7.0) upon adding of an increasing concentration of A-4 from 0 to 55.5 equiv. Inset: A plot of absorption spectroscopy intensity as estimated by the peak height at 293 nm.

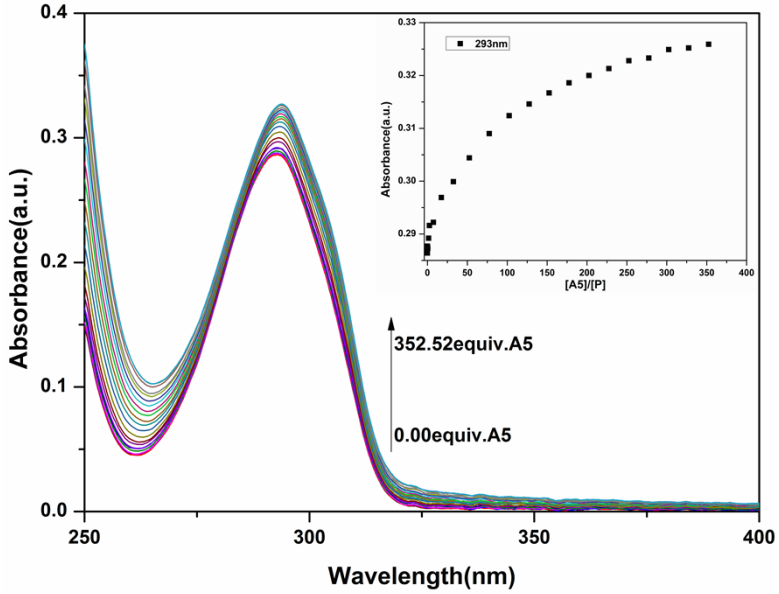

Fig. S36. UV-vis spectra of **P** (20μM) in H_2O (pH=7.0) upon adding of an increasing concentration of A-5 from 0 to 352.5 equiv. Inset: A plot of absorption spectroscopy intensity as estimated by the peak height at 293 nm.

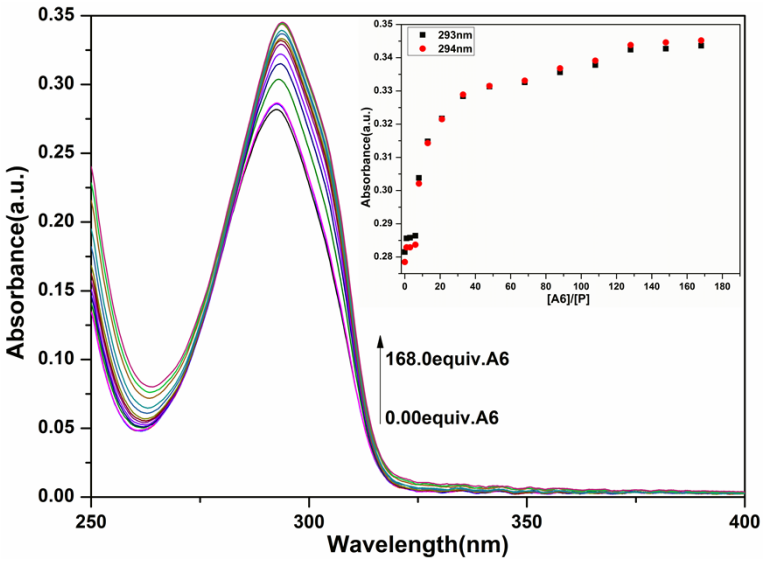

Fig. S37. UV-vis spectra of **P** (20μM) in H_2O (pH=7.0) upon adding of an increasing concentration of A6 from 0 to 168 equiv. Inset: A plot of absorption spectroscopy intensity as estimated by the peak height at 293 and 294 nm.

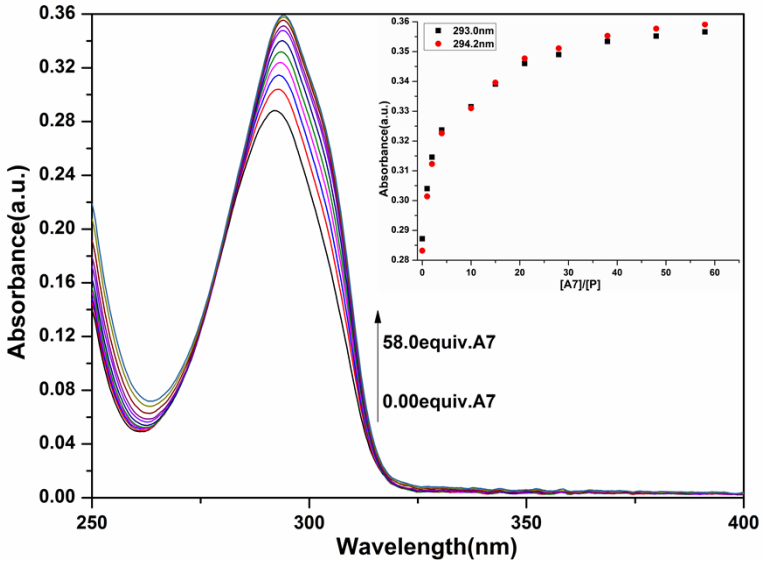

Fig. S38. UV-vis spectra of **P** (20μM) in H_2O (pH=7.0) upon adding of an increasing concentration of A7 from 0 to 58 equiv. Inset: A plot of absorption spectroscopy intensity as estimated by the peak height at 293 nm.

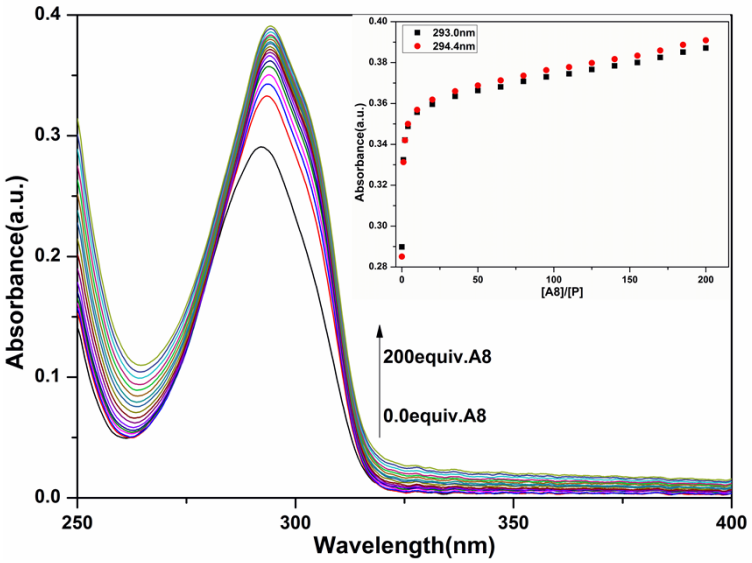

Fig. S39. UV-vis spectra of **P** (20μM) in H_2O (pH=7.0) upon adding of an increasing concentration of A8 from 0 to 200 equiv. Inset: A plot of absorption spectroscopy intensity as estimated by the peak height at 293 nm.

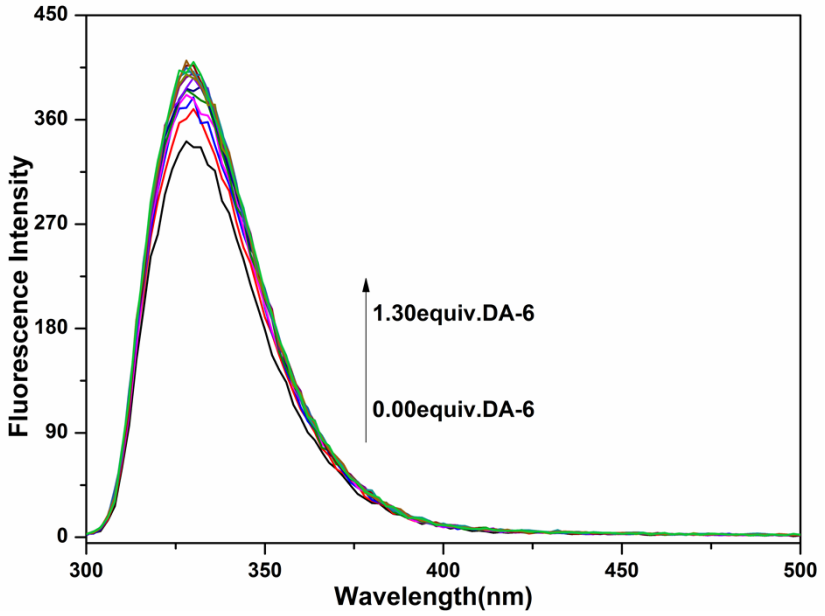

Fig. S40. Fluorescence titrition spectra of **P** (20 μM) in H_2O (pH=7.0) upon adding an increasing concentration of DA-6 from 0 to 1.3 equiv.(λ_{ex}=293 nm).

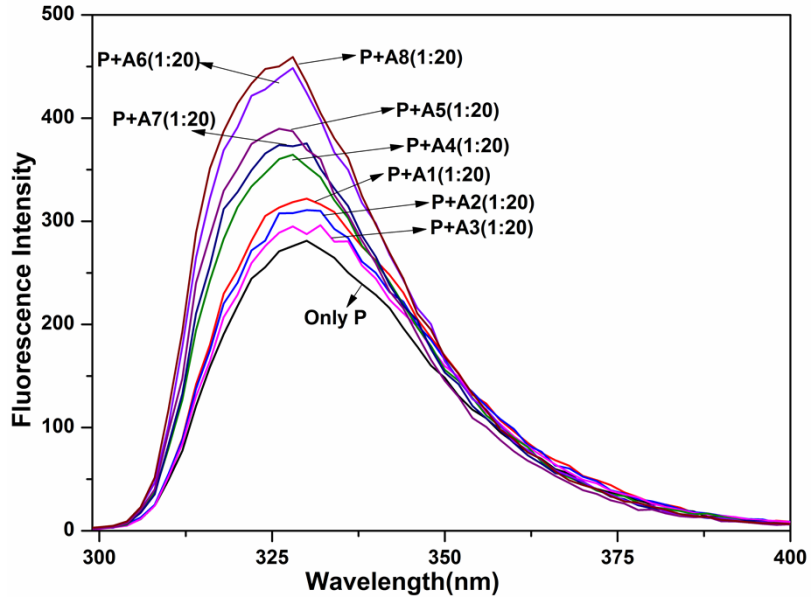

Fig. S41. Fluorescence spectra response of P (20 μM) upon addition of A1, A2, A3, A4, A5, A6, A7 and A8 (20 equiv.) in H_2O (pH=7.0), (λ_{ex}=293 nm).

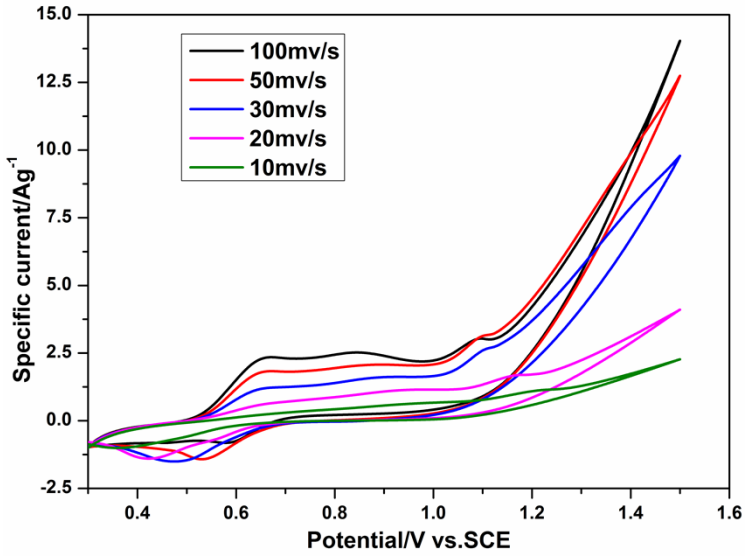

Fig. S42. Cyclic voltammograms of host **P** (0.33mM) recorded at different scan rates in H_2O (pH=7.0).

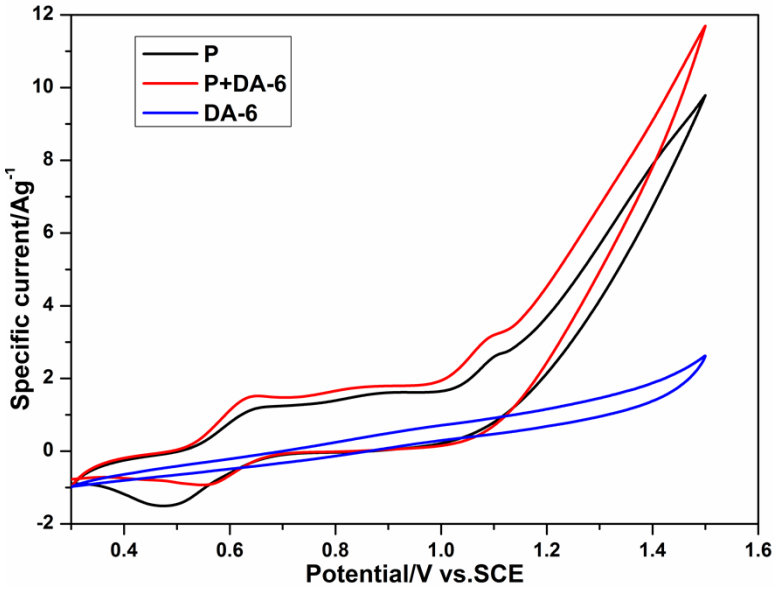

Fig. S43. Cyclic voltammograms of **P** (0.33 mM) in H_2O solutions in the absence and the presence of DA-6 (10.1mM). Scan rate = 30 mV/s.